

ELECTRONICALLY CONTROLLED INERTIA FOR LABORATORY TESTING OF TRACTOR BRAKES AND CLUTCHES

*A dissertation
submitted in partial fulfillment of the requirements
for the degree of*

Master of Technology

by

Chaitanya J. Diwan
(Roll No. 04307421)

under the supervision of
Prof. L. R. Subramanyan & Prof. P. C. Pandey



Department of Electrical Engineering

Indian Institute of Technology Bombay

July 2007

Chaitanya J. Diwan / Prof. L. R. Subramanyan & Prof P. C. Pandey (Supervisors),
“Electronically controlled inertia for laboratory testing of tractor brakes and clutches”,
M.Tech. dissertation, Department of Electrical Engineering, Indian Institute of
Technology Bombay, July 2007.

ABSTRACT

On-road evaluation of tractor brakes and clutches is a time consuming process and has other shortfalls like unsafe riding conditions, less repeatability and limitation of brake input force, requirement of special track etc. In test rigs for laboratory testing of brakes and clutches, tractor and trailer inertia is simulated by using flywheels. In these setups, it is difficult to simulate the variable inertia representing different tractor ballast conditions, and rotating mass of the flywheel can lead to unsafe operating conditions and frequent maintenance of the test rig. The objective of this project is to develop a test rig, with the help of a separately excited dc motor and electronic monitoring and control unit, which simulates variable moment of inertia, damping, and friction for a realistic testing of brakes and clutches. Instantaneous speed is sensed and used for giving control voltage to motor drive to generate the instantaneous value of the torque as required for simulating inertia, damping, and friction. Brake application is controlled through a solenoid. Cumulative energy dissipated in brake is calculated from instantaneous values of speed, torque, and brake application time, and energy dissipated per application can be controlled. Test set up has been developed for endurance and performance testing of brake, using a 746 W (1 H. P.) motor for concept demonstration. The electronic monitoring and control setup can be used, with the help of higher power motor and drive, for testing of tractor brakes and clutches.

CONTENTS

| | |
|---|-------------|
| Abstract | iii |
| List of symbols | vi |
| List of abbreviations | vii |
| List of figures | viii |
| List of tables | x |
| Chapters | |
| 1. Introduction | 1 |
| 1.1 Overview | 1 |
| 1.2 Project objectives | 1 |
| 1.3 Outline of the dissertation | 2 |
| 2. Testing of tractor brakes and clutches | 3 |
| 2.1 Tractor evaluation | 3 |
| 2.2 Tractor brake | 3 |
| 2.3 Tractor clutch | 7 |
| 2.4 Track testing of tractor brakes and clutches | 8 |
| 2.5 Energy dissipated in tractor brakes and clutches during haulage operation | 8 |
| 2.6 Laboratory testing of tractor brakes and clutch | 10 |
| 3. Electronically controlled test system | 13 |
| 3.1 Torques on tractor engine and brake | 13 |
| 3.2 Inertia test system | 15 |
| 3.3 Hardware development | 15 |
| 3.4 Software development | 25 |
| 3.5 Inertia logic development | 28 |
| 3.6 Development of control system | 29 |
| 3.7 Software architecture | 31 |
| 3.8 Integration and debugging | 36 |

| | |
|--|-----------|
| 3.9 Testing and qualification | 38 |
| 3.10 Sampling frequency selection | 38 |
| 3.11 Modification of setup for experimental validation | 41 |
| 4. Tests and results | 44 |
| 4.1 Introduction | 44 |
| 4.2 Test I: Comparison of ECI and MI setup | 45 |
| 4.3 Test II: Effect of variation in inertia | 49 |
| 4.4 Test III: Effect of variation in speed | 51 |
| 4.5 Test IV: Effect of variation in energy | 52 |
| 4.6 Test V: Effect of variation in friction | 53 |
| 4.7 Test VI: Effect of variation in damping | 54 |
| 5. Summary and conclusions | 56 |
| Appendices | 58 |
| A. Data acquisition card and drive unit | 58 |
| B. Testing of data acquisition card | 60 |
| C. Assembly of test system | 64 |
| D. Brake testing cycle based on IS: 12061-1994 for Mahindra & Mahindra tractor | 66 |
| Acknowledgements | 67 |
| References | 68 |

LIST OF SYMBOLS

| Symbols | Explanation |
|----------------|--|
| a | Deceleration |
| b | Damping constant |
| f_s | Sampling frequency |
| J | The inertia to be simulated in inertia dynamometer |
| K_1 | Voltage to speed ratio |
| K_2 | Speed to torque ratio of motor |
| r_{xy} | Correlation coefficient of data sets x , and y |
| T_b | Brake torque |
| T_d | Damping torque |
| T_e | Engine torque |
| T_f | Friction constant |
| T_{fr} | Friction torque |
| T_g | Gravitational torque |
| T_{gm} | Gravitation constant |
| T_i | Inertial torque |
| T_m | Maximum torque of the motor used in setup |
| T_s | Set torque demand |
| t_{eb} | Braking time |
| t_{es} | Time elapsed after starting the test |
| t_{ab} | Set time delay for application of brake |
| t_b | Maximum brake application time |
| ε | The mean of magnitude of differences |

LIST OF ABBREVIATIONS

| Abbreviation | Explanation |
|---------------------|-----------------------------------|
| PC | Personal computer |
| PCI | Peripheral component interconnect |
| HDD | Hard disk drive |
| RAM | Random access memory |
| AI | Analog input |
| AO | Analog output |
| DO | Digital output |
| DSO | Digital storage oscilloscope |
| DAC | Data acquisition card |
| A/D | Analog-to-digital converter |
| D/A | Digital-to-analog converter |
| I/O | Input and output |
| ECI | Electronically controlled inertia |
| MI | Mechanical inertia |

LIST OF FIGURES

| | | |
|------|---|----|
| 2.1 | Schematic diagram of a tractor brake system | 4 |
| 2.2 | Typical graph showing wear characteristics of brake liner material | 6 |
| 2.3 | A typical performance mapping during endurance test | 6 |
| 2.4 | A typical speed mapping with respect to time during burnishing test | 7 |
| 2.5 | Single plate clutch | 7 |
| 2.6 | Power train and transmission design for four wheel drive tractor | 8 |
| 2.7 | Block diagram of inertia dynamometer | 12 |
| 3.1 | Block diagram of the proposed electronically controlled setup | 16 |
| 3.2 | Separately excited dc motor diagram | 17 |
| 3.3 | Photograph of separately excited dc motor used in the setup: Separately excited dc motor of make “Librathern” model 2K6, 0.746 kW (1 H. P.) | 18 |
| 3.4 | Photograph of speed measurement arrangement | 18 |
| 3.5 | Block diagram of frequency-to-voltage converter [Librathern, model ISM - 10] | 19 |
| 3.6 | Photograph of brake fixing on the motor shaft | 20 |
| 3.7 | Photograph of mechanical setup of test system | 20 |
| 3.8 | Wiring diagram of drive of make Librathern, model TDM - 1000 | 22 |
| 3.9 | Block diagram of isolator of make Librathern, model ISM - 10 | 23 |
| 3.10 | Solenoid driver circuit developed | 24 |
| 3.11 | Photograph of industrial computer of make Dynalog, model IPC - 611 | 24 |
| 3.12 | Photograph of terminal block to interface data acquisition card NI 6221 with electronic system junction box1 | 25 |
| 3.13 | Module 1 for controlling set speed before application of brake | 34 |
| 3.14 | Module 2 for controlling energy dissipated in brake | 35 |
| 3.15 | Photograph of test setup developed | 36 |
| 3.16 | Photograph of electronic system developed for test system | 37 |

| | | |
|------|---|----|
| 3.17 | Photograph of test setup developed for endurance testing of brake | 37 |
| 3.18 | Photograph of test setup with flywheel mounted for verification of the system | 42 |
| 3.19 | Photograph of modified test setup to carry out experiment with different sizes of flywheel and electronic test system | 42 |
| 4.1 | Measured results of Test No. 1 | 46 |
| 4.2 | Measured results of Test No. 2 | 47 |
| 4.3 | Measured results of Test No. 3 | 48 |
| 4.4 | Graph of moment of inertia vs. braking time | 50 |
| 4.5 | Graph of speed vs. braking time | 51 |
| 4.6 | Graph of energy vs. braking time | 53 |
| 4.7 | Graph of friction vs. braking time | 54 |
| 4.8 | Graph of damping vs. braking time | 55 |
| A.1 | 68 pin D connector details of data acquisition card NI 6221(from National Instruments) | 58 |
| A.2 | Photograph of data acquisition card, National Instrument model NI 6221 | 59 |
| A.3 | Drive for separately excited dc motor, Libratherm model TDM - 1000 | 59 |
| B.1 | Testing of analog input in NI 6221 driver software | 61 |
| B.2 | Testing of analog output in NI 6221 driver software | 62 |
| B.3 | Testing of digital I / O lines in NI 6221 driver software | 63 |

LIST OF TABLES

| | | |
|-----|--|----|
| 2.1 | List of typical values of mass, wheel dimension, speed etc for the tractor “Model 575” with trolley of make Mahindra and Mahindra | 10 |
| 2.2 | Calculated values of angular velocity, deceleration, and stopping time etc during haulage operation of the tractor | 10 |
| 3.1 | Specifications of 746 W separately excited dc motor used in test setup | 17 |
| 3.2 | Input control voltages, observed voltage across dc drive and motor speed relationship | 21 |
| 3.3 | Relationship between input voltage and output voltage of the analog optoisolator | 23 |
| 3.4 | List of sensed and set parameters, input through ADC channels | 27 |
| 3.5 | Test system parameter. | 30 |
| 3.6 | Combination of values of inertia, damping, and friction, angular speed in different tests | 39 |
| 3.7 | Braking time at different sampling frequency for tests involving a combination of values of inertia, damping, and friction and angular speed | 40 |
| 3.8 | Correlation coefficients between sampling frequency pairs, for braking time | 40 |
| 3.9 | The mean of magnitude of differences between sampling frequency pairs, for braking time | 41 |
| 4.1 | Results of Test I: Braking time with flywheel and with test system for different values of inertia, angular speed and energy levels | 45 |
| 4.2 | Results of Test II: Braking time t_{eb} for different values of moment of inertia J , for a given set of E_s, N_s, b, T_f | 49 |
| 4.3 | Results of Test II: Calculated parameters (total energy, residual energy) and recorded readings (energy dissipated in brake and residual energy) for different values of moment of inertia J , for a given set of E_s, N_s, b, T_f | 50 |
| 4.4 | Results of Test III: Braking time t_{eb} for different values of speed N_s , for a given set of E_s, J, b, T_f | 51 |

| | | |
|-----|--|----|
| 4.5 | Results of Test III: Calculated parameters (total energy, residual energy) and recorded readings (energy dissipated in brake and residual energy) for different values of speed N_S , for a given set of E_S, J, T_f | 52 |
| 4.6 | Results of Test IV: Braking time t_{eb} for different values of energy E_S , for a given set of N_S, J, b, T_f | 52 |
| 4.7 | Results of Test IV: Calculated parameters (total energy, residual energy) and recorded readings (energy dissipated in brake and residual energy) for different values of energy E_S , for a given set of N_S, J, T_f | 53 |
| 4.8 | Results of Test V: Braking time t_{eb} for different values of friction constant T_f , for a given set of N_S, J, b, E_S | 54 |
| 4.9 | Results of Test VI: Braking time t_{eb} for different values of damping b , for a given set of N_S, J, T_f, E_S | 55 |
| C.1 | Component list of test system | 64 |

Chapter 1

INTRODUCTION

1.1 Overview

Tractors are used for various agricultural and non-agricultural applications, including land and soil preparation, harvesting, irrigation by running pumps, goods transport for short distances, and low cost construction equipment [1], [2]. The usage pattern largely depends on type of operation, region, and operator driving habits. This large range of usage pattern poses many challenges for tractor testing and evaluation. On-road testing of prototype tractor is expensive because it comprises many prototype subsystems. If one of these subsystems fails during testing, the other subsystems cannot be tested without it. It is possible to eliminate this interdependence of subsystems by testing these subsystems and components independently in the laboratory. For example, a prototype transmission can be evaluated without prototype engine attached to it, so that the engine problems need not affect the transmission test schedule. The evaluation process starts with field load data acquisition, followed by development of test load cycles and test facilities to simulate the field load conditions in the laboratory.

1.2 Project objectives

Proper functioning of brake and clutch is essential for most of the tractor applications like haulage, cultivation, puddling, construction, etc. Both being wearable parts, their performance testing is important. Brake performance primarily measures stopping distance, and brake output torque [1] - [4]. Normal laboratory testing for clutch and brake system is inertia dynamometer [5] - [7] equipped with a drive motor and a detachable flywheel which stores the kinetic energy equivalent to that of the tractor in motion. The accuracy of the inertia simulation is not precise because it is adjusted by

varying the fixed mass of flywheel. Further the rotating flywheel is unsafe at higher speed. Wear and tear of mechanical parts, lead to frequent breakdown of the test rig. In this setup, the testing time is relatively more as the system has to accelerate the mass to reach the test speed during each cycle. Further, it is very difficult to simulate the frictional and damping forces which are invariably present during actual braking.

The project objective is to develop an electronically controlled set-up for testing of brake with the following features

- (a) Simulation of variable inertia, damping, and friction.
- (b) Elimination of risks due to rotating mass.
- (c) Electronic control of energy dissipated per braking cycle or in a specified time.
- (d) Faster testing as compared to flywheel based inertia dynamometer.

This system can also be used for clutch testing.

1.3 Outline of the dissertation

Chapter 2 gives an overview of different methods that are used to develop inertia. It gives an overview of the tractor brakes and clutches, evaluation of tractor, track testing of tractor brake and clutch. It describes energy dissipated in brake, inertia, stopping time calculation required for tractor to dissipate the energy in the brake, and traditional brake testing system. Chapter 3 describes the concept of development of electronically controlled variable inertia. It explains the development stages of inertia test system: hardware development, software development, and integration and testing. It describes the hardware modules: current-to-voltage converter, signal isolator, frequency-to-voltage converter, and drive unit for separately excited dc motor, mounting of brakes, development of mechanical model of the test system unit, interfacing of the data acquisition card to computer. It describes software modules: graphical user interface panels, configuration of channel, and development of control system algorithm, graphical representation of speed and torque along with time, data acquisition of test data, alarm configuration for safety of device and test component. It describes integration and testing to develop the complete inertia test system. Chapter 4 gives the test results for different test conditions. Chapter 5 summarizes the work along with some suggestions for further work. Appendices provide supplementary information: data acquisition card connector details, test panels for testing of data acquisition card, component list, brake testing cycle based on IS: 12061-1994.

Chapter 2

TESTING OF TRACTOR BRAKES AND CLUTCHES

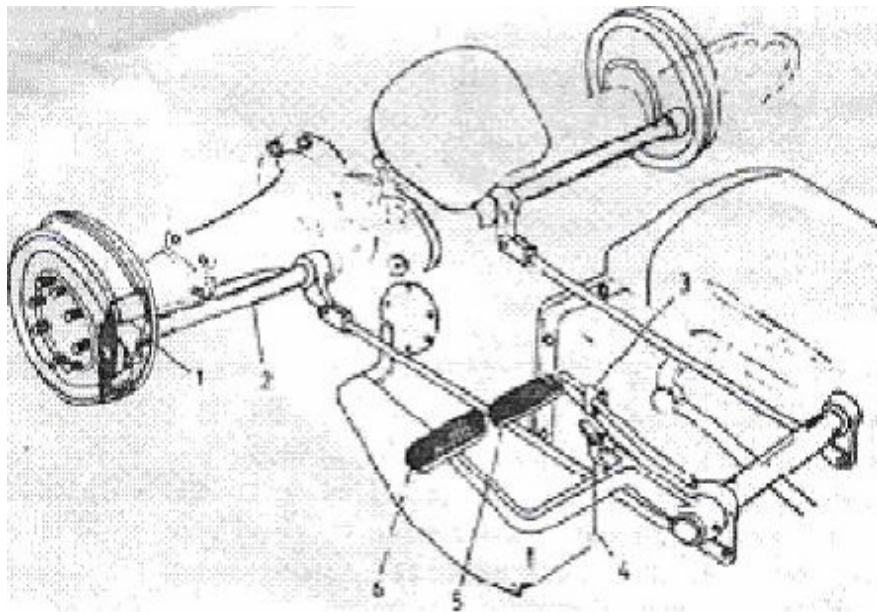
2.1 Tractor evaluation

Tractors are evaluated through laboratory testing, field testing, track testing, and computer simulation. Advantages of laboratory testing are good repeatability, reliability, possibility of accelerated testing, and close monitoring of testing. Disadvantages of laboratory testing are: (i) it requires costly infrastructure, (ii) exact field simulation may not be possible, and (iii) effect of environmental conditions may not be properly simulated. Field testing is close to the customer usage pattern and under actual environmental conditions. But it is time consuming and expensive. Further, repeatability and reliability are low. Track testing gives better repeatability and conditions are closer to the customer usage. Disadvantages of track testing are: structural loading and accelerated test for limited components, high infrastructure cost. Computer simulation permits faster evaluation in a cost effective way and more designs can be evaluated. However, accuracy of the test results is limited by accuracy of input data and the actual subsystems can not be tested.

2.2 Tractor brake

The function of the brake system in a tractor is to bring it to a stop or slow down its motion. The system is mounted on the driving axle and it is operated by two independent pedals situated on the right hand side of the transmission case as shown in Fig. 2.1. Each pedal can be operated independently or locked together by means of a lock. The principle of operation is based on friction between moving elements brought in contact with stationary element. The motion is opposed by the frictional force, which acts in the opposite direction of the motion and converts kinetic energy to heat energy.

The magnitude of friction depends upon the type and quality of the surfaces in contact and the pressure.



1 - Brake shoe 2 - Actuating case 3 - Parking latch 4 - Interlocking latch
5 - Left hand side brake pedal 6 - Right hand side brake pedal

Fig. 2.1 Schematic diagram of a tractor brake system [4].

Types of mechanical brakes are internal expanding shoe brakes, external contracting shoe brakes, and disc brakes [4]. The two brake shoes are made of frictional material fitted on the inside of the drum and are held away from the drum by means of springs. One end of each shoe is pivoted, whereas the other is free to move by action of a cam, which in turn applies force on shoes. The brake pedal through the linkage causes the movement of the cam. The drum is mounted on the rear axle, whereas the shoe assembly is stationary and mounted on the back plate. Brakes are designed to withstand a lot of heat, but too much heating of the brake assemblies can eventually decrease their ability to stop the tractor. The loss of braking capacity on long steep downgrades is due to combined effect of heating, brake system design, friction material properties, and brake adjustment [7] - [11].

The tests carried out for the evaluation of brake system are lever deflection test, endurance test, performance test, downhill mode test, burnishing test to study wear characteristics, and temperature mapping test [7].

2.2.1 Lever deflection test

This test helps in validation of brake lever movement to the input force applied. In this test, excess free play and transmission loss in linkages can be determined. Input for this test is maximum force to be applied on the brake pedal.

2.2.2 Endurance test

Endurance test is conducted to determine the life of brake system, which mainly depends on the wear characteristics of friction material used in brake liners. Endurance test conducted on road is a time consuming process and it has several drawbacks like limitations on maximum force, repeatability, maintaining test speed etc. Fig. 2.2 shows a typical plot of wear characteristics of brake liner material for endurance testing of three different liner materials.

2.2.3 Performance test

Stopping distance is one of the important measures of brake performance. Performance tests are conducted at various input forces for different initial speed. The input parameters for performance test are vehicle mass, tyre diameter, brake input force, cooling time, etc. Performance of brake system mainly depends on the liner characteristics of fiber, resin, and filler materials which are used in the base composition of friction material. Based on performance test, friction coefficient of liner material can also be determined. Stopping distance is analyzed from performance test results. This analysis helps in comparing the performance characteristics of different brake drum materials much easier and faster. A typical performance characteristic is shown in Fig. 2.3.

2.2.4 Downhill mode test

Road condition varies from place to place. For example, flat straight road in case of highways, more steep gradients in case of hilly regions etc. Driving pattern will vary depending upon the skill of the driver. Generally beginners will drive at less speed with brakes online. In case of hilly regions, drivers are forced to apply brakes continuously or very frequently. Such conditions are also considered in brake testing. Temperature is monitored on the surface of brake drum thorough a non-contact temperature sensor. After completion of test, the brake friction material is inspected.

2.2.5 Burnishing test

Burnishing test for any liner is conducted to ensure effective contact to the brake drum. Generally burnishing test is conducted at a lower deceleration. During burnishing test, distance between every successive braking is kept 1000 m as shown in Fig. 2.4.

2.2.6 Temperature mapping test

Brake liner material behavior changes adversely with respect to temperature. Brake performance drops drastically at elevated temperatures. This depends on the temperature withstanding capacity of the base fiber material used in the liner.

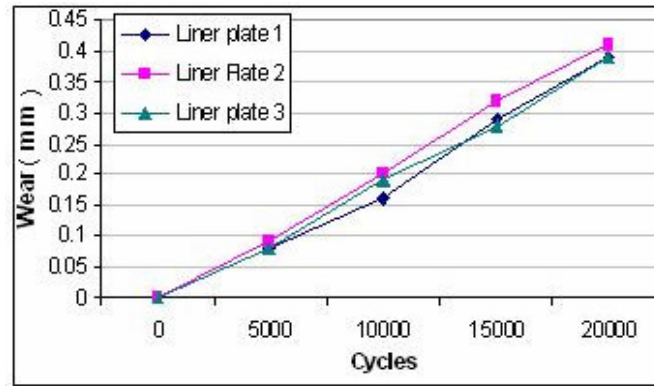


Fig. 2.2 Typical graph showing wear characteristics of brake liner material [7]

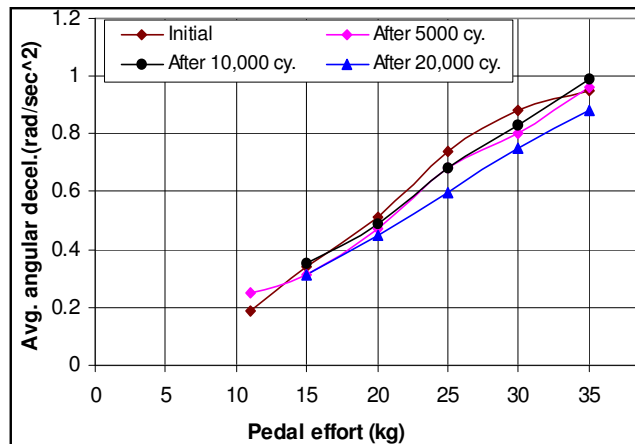


Fig. 2.3 A typical performance mapping during endurance test [7]

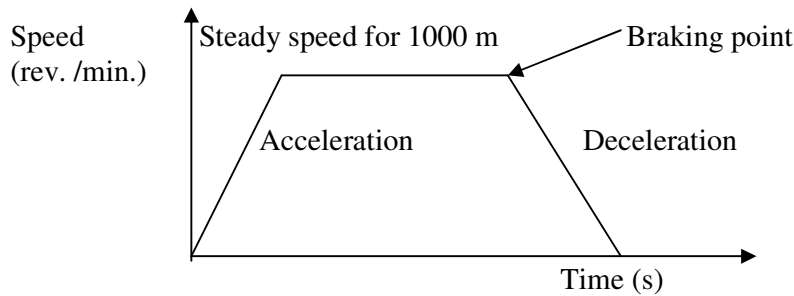


Fig. 2.4 A typical speed mapping with respect to time during burnishing test [7].

2.3 Tractor clutch

The internal combustion engine must be cranked manually or by a special starting mechanism. This type of engine must attain a certain speed before it can be loaded. Hence during starting of the engine, the power unit has to be disconnected from the transmission gears and drive wheels of tractor. Shifting of the transmission gears must be permitted for the purpose of securing different travelling speeds and stopping the belt pulley must be permitted without having to stop the engine [2]. All these are taken care of by placing a clutch between the engine and the transmission gears and belt pulley.

A single plate clutch with two friction surfaces is shown in Fig. 2.5. The power train and transmission cross section for a four wheel drive tractor is shown in Fig. 2.6. Power is first transmitted to two sets of primary master gears. These gears, in turn, transmit power to two sets of change speed gears by which the different travel speeds are obtained. These gears then transmit the power to the front and rear final drive gears and axles.

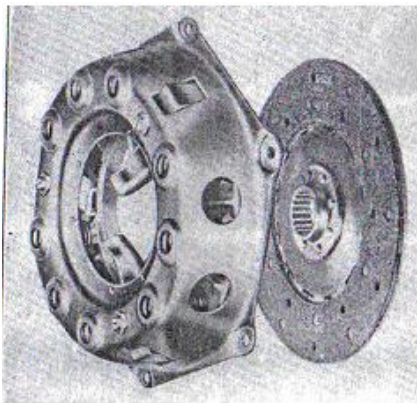


Fig. 2.5 Single plate clutch [4].

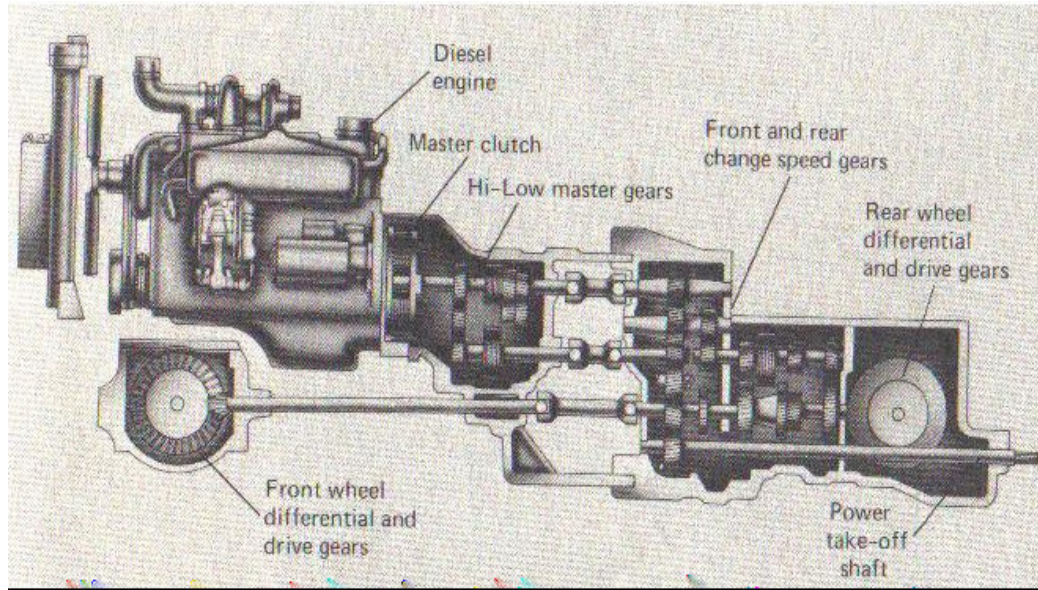


Fig. 2.6 Power train and transmission design for four wheel drive tractor [2].

2.4 Track testing of tractor brakes and clutches

In track testing [1], speeds of the four wheels of tractor are recorded. A fifth wheel is attached to measure the stopping distance. Proximity switch is connected to the fifth wheel to measure the number of pulses. Load cell is attached to brake pedal. It is electronically coupled with the brake pedal load cell. Brake pedal force increased to a certain limit will trigger the electronic circuit to count the number of rotation of the fifth wheel. Stopping distance is calculated from the number of counts multiplied by the circumference of the wheel. Stopping time, brake pedal force and rear axle speed of a tractor are simultaneously recorded during checking performance of tractor brakes.

2.5 Energy dissipated in tractor brakes during haulage operation

Calculation of moment of inertia, drive shaft speed, stopping time, and typical values of energy dissipated in brake and clutch during haulage operation is described here. Independent variables used in the calculation along with their typical values for a specific tractor model are given in Table 2.1.

From the speed s_k given in km/hr, we calculate the speed of the tractor s_m in m/s as

$$s_m = s_k (1000 / 3600) \quad (2.1)$$

Angular speed of the wheel ω_a in rad/s is calculated from linear speed s_m in m/s and wheel radius r in m as

$$\omega_a = s_m / r \quad (2.2)$$

The axle speed N_1 in rev. /min. is calculated from linear speed s_m in m/s and wheel radius r in m as

$$N_1 = 60 s_m / (2 \pi r) \quad (2.3)$$

Drive shaft speed N_2 in rev. /min. is calculated from axle speed N_1 in rev. /min. and gear ratio g_a

$$N_2 = g_a N_1 \quad (2.4)$$

Assuming a constant deceleration over the stopping distance, the deceleration a in m/s^2 is calculated from linear speed s_m in m/s and stopping distance d_s in m as

$$a = 0.5 s_m^2 / d_s \quad (2.5)$$

The stopping time t_s in s is calculated from linear speed s_m in m/s and deceleration a in m/s^2 as

$$t_s = s_m / a \quad (2.6)$$

Kinetic energy E_k in J is calculated from total mass of tractor and trolley m_{tt} in kg and linear speed s_m in m/s as

$$E_k = 0.5 m_{tt} s_m^2 \quad (2.7)$$

The kinetic energy of the tractor is to be absorbed by the brake assembly during braking. Energy absorbed per brake E_b in Joules (J) is the total kinetic energy divided by the number of brakes n_b in the assembly. Power absorbed by the brake assembly P in W is calculated from energy absorbed E_k in J and stopping time t_s is

$$P = E_k / t_s \quad (2.8)$$

Using the values for a specific model listed in Table 2.1, values of the parameters given by (2.1) - (2.8) were calculated and these are listed in Table 2.2.

Table 2.1 List of typical values of mass, wheel dimension, speed etc for the tractor “Model 575” with trolley of Mahindra and Mahindra. make

| Sl. No. | Parameter | Symbol | Value | Unit |
|---------|---|----------|-------|-------|
| 1 | Mass of tractor | m_t | 4890 | kg |
| 2 | Total mass of tractor and trolley | m_{tt} | 24890 | kg |
| 3 | Rolling radius of wheel | r | 0.69 | m |
| 4 | Stopping distance | d_s | 10 | m |
| 5 | Gear ratio of drive shaft speed to axle speed | g_a | 18 | - |
| 6 | Tractor speed | s_k | 15 | km/hr |
| 7 | Number of brakes | n_b | 2 | - |

Table 2.2 Calculated values of angular velocity, deceleration, and stopping time etc during haulage operation of the tractor with parameters as given in Table 2.1

| Sl. No. | Parameter | Symbol | Value | Unit |
|---------|---------------------------------------|------------|--------|------------------|
| 1 | Linear speed of the tractor | s_m | 4.17 | m/s |
| 2 | Angular speed | ω_a | 6.04 | rad/s |
| 3 | Axle speed | N_1 | 57.59 | rev./min. |
| 4 | Drive shaft speed | N_2 | 1041 | rev./min. |
| 5 | Deceleration | a | 0.87 | m/s ² |
| 6 | Stopping time | t_s | 4.80 | s |
| 7 | Kinetic energy due to linear velocity | E_k | 216000 | J |
| 8 | Power absorbed in brake assembly | P | 45000 | W |

2.6 Laboratory testing of tractor brakes and clutch

In laboratory, testing of brake and clutch system is conducted using inertia dynamometer [5] - [7] equipped with a drive motor and a detachable flywheel, which represents the moving mass of the tractor, as shown in Fig. 2.7. For simulating the road condition for brake application, the drive motor is coupled with transmission unit where the brakes are fitted. Drive shaft speed, kinetic energy, stopping time, and total energy dissipated in brake are calculated as per the equations in previous sections. The moment

of inertia of the flywheel should be such that when its speed becomes equal to the speed of the tractor drive shaft, its kinetic energy equals the kinetic energy to be dissipated by the brake assembly i.e. E_k .

The net inertia J in kg m^2 to be simulated in inertia dynamometer is calculated from the total energy E_k in J and angular speed of drive shaft ω_a is rad/s as

$$J = E_k / (0.5 \omega_a^2) \quad (2.9)$$

Moment of inertia of the flywheel in inertia dynamometer J_f in kg m^2 is calculated from the net moment of inertia J in kg m^2 and moment of inertia of the assembly of the inertia dynamometer J_s in kg m^2 as

$$J_f = J - J_s \quad (2.10)$$

Radius of flywheel r_f in m is calculated from the net moment of inertia to be simulated in laboratory J_f in kg m^2 and mass of flywheel m_f in kg as

$$r_f = \sqrt{(2J_f / m_f)} \quad (2.11)$$

Based on these calculations, the size of flywheel is selected and fitted at the end of drive motor for simulation of moment of inertia and evaluation of the brake performance.

The test system follows the following sequence, with brake assembly in released condition, speed of the electric motor driving the shaft is increased. When the required drive shaft speed is reached, the control system removes the signal of the drive and brakes are applied. When drive shaft speed becomes zero, brakes are released and the same cycle is repeated again for a predefined number of cycles.

The basics of the moment of inertia, damping force, and friction force are discussed in [5], [7], and [12] - [18]. Development of variable inertia using a mechanical flywheel is discussed in [5], [7]. Concept of a flexible flywheel for internal energy storage for home or farm use is discussed in [19]. Advantages of this concept are self balancing due to highly flexible rotor operating at supercritical speeds, low cost, safety in use, simple construction, lower operating speeds and lower power losses than conventional high performance flywheels. An analog simulation of a flywheel propulsion system for buses is discussed in [20]. The paper presents the techniques used in an analog simulation of a flywheel energy storage drive system, in which the electrical components such as the thyristors of the converter, the controller, and the electrical machines are simulated in detail. Variable inertia generation using dynamometers is discussed in [5], [7], and [21] - [24].

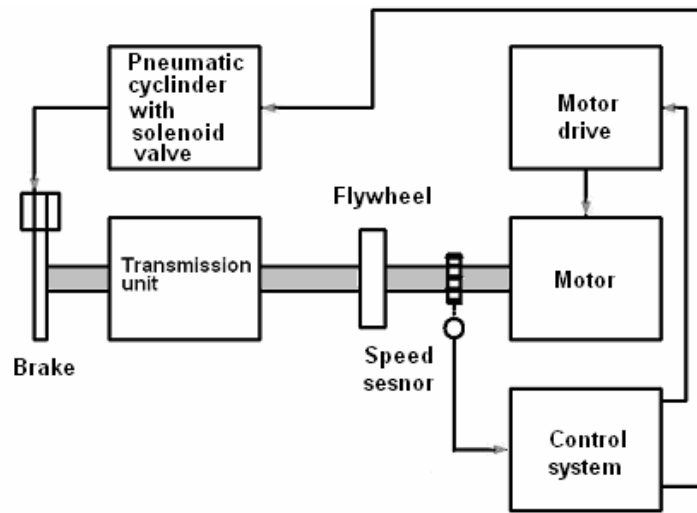


Fig. 2.7 Block diagram of inertia dynamometer.

In an inertia dynamometer with flywheel, it is unsafe to rotate the mass at higher speed and there is high wear and tear of the system. Further with this facility, it is difficult to generate the variable inertia as it involves changing the flywheel. Also we can not simulate road inclination, damping, and friction. In order to overcome the above said drawbacks of the inertia dynamometer with flywheel, there is a need to develop a test bench which can develop variable inertia, damping force, and friction force. No test system has been reported which generates electronically controlled variable moment of inertia, damping force, and friction for testing tractor brakes and clutches. Our objective is to develop such a system for laboratory testing of tractor brakes and clutches.

Chapter 3

ELECTRONICALLY CONTROLLED TEST SYSTEM

3.1 Torques on tractor engine and brake

The total torque T_e coming on tractor engine is sum of the torque due to inertia T_i , torque due to damping force T_d , torque due to kinetic friction T_{fr} , torque due to brake T_b , and torque due to gravitation T_g

$$T_e = T_i + T_d + T_{fr} + T_b + T_g \quad (3.1)$$

For angular velocity ω and rotational moment of inertia J , the moment of inertia torque T_i is given as

$$T_i = J \frac{d\omega}{dt} \quad (3.2)$$

Nature of the frictional force between two given surfaces depends on the surface condition, the pressure between the surfaces and their relative velocity. The friction acts in a direction opposite to that of velocity. Static friction occurs when the two objects are not moving relative to each other. Kinetic friction occurs when two objects are moving relative to each other and rub together. The torque T_{fr} due to kinetic friction can be given as

$$T_{fr} = T_f, \text{ if } \omega > 0 \\ - T_f, \text{ if } \omega < 0 \quad (3.3)$$

The friction torque T_{fr} represents the torque due to road friction as well as friction due to various moving parts.

Damping torque may be modeled as being proportional to the instantaneous velocity and in the opposite direction to it. For angular velocity ω and damping constant b , the damping torque may be approximated as

$$T_d = b\omega \quad (3.4)$$

The torque due to gravitation depends on the angle of inclination α

$$T_g = T_{gm} \sin(\alpha) \quad (3.5)$$

It is positive for uphill slope and negative for downhill slope and zero on a level road.

During brake testing, we normally assume that the engine is turned off and the road is level, i.e. $T_e = 0$ and $T_g = 0$. In an inertia dynamometer for brake testing as shown earlier in Fig 2.7, the brake assembly to be tested is attached to a shaft coupled to a flywheel and a motor. The moment of inertia of the flywheel together with that of the shaft simulates the inertia of the moving tractor mass. The motor is used as the prime mover. The motor is started and kept running until the desired angular speed is achieved. At this instant the kinetic energy in the rotating mass represents the energy in the moving tractor. The motor is turned off and the brake is applied. The kinetic energy in the rotating mass is dissipated by the brake and the shaft comes to rest. This test cycle is repeated as per test requirements. In this system, energy dissipated per cycle is fixed. We can monitor the time taken in successive application of the brake. One of the advantages of this setup is that a relatively low power motor can be used for storing energy in the flywheel.

In place of a fixed flywheel, we can use a separately excited dc motor to develop the torque as given by (3.2). The control output for varying the armature voltage can be selected such that the torque developed is proportional to angular deceleration. The motor is first used as prime mover to achieve the test speed. At this instant, the brakes are applied and the motor drive switches to inertia simulation mode. The torque developed by the motor can be varied to also simulate the sum of desired values of other torques in (3.1).

The net torque seen by the brake is

$$T_b = T_e - T_i - T_d - T_{fr} - T_{gm} \quad (3.6)$$

By taking $T_{gm} = 0$ and $T_e = 0$, and T_i and T_d as given by (3.2) and (3.4) we get

$$T_b = -J \frac{d\omega}{dt} - b\omega - T_{fr} \quad (3.7)$$

This torque has to be dynamically varied by varying the armature supply of the motor, and can be realized by having a setup that can sense the angular speed ω , calculate the angular deceleration, and having a variable armature drive with fast response time.

3.2 Inertia test system

Proposed setup, with the brake to be tested coupled to the shaft of the motor, is shown in Fig. 3.1. The dc drive gives constant supply V_f to field winding and variable supply V_a to armature winding of the motor. A current sensor is used to sense the armature current of motor and give feedback to software for torque control. Speed sensor gives speed feedback to control the speed of the motor. A computer, with A/D inputs and D/A output, is used for controlling the motor drive. Optoisolators are used to isolate the control signals from computer to the motor drive. Torque demand is derived from the set values of damping constant, friction, moment of inertia, and the sensed angular velocity. At the start of a test cycle, the motor is given drive to start rotating and reach set speed with preset acceleration. When the set speed is reached, brake is applied and the shaft starts decelerating. During haulage operation in the field, a typical value of energy dissipated in brake assembly is 216 kJ in 5 s (ref. Table 2.2) with an average power of 45 kW. Hence to have an electronically controlled simulation inertia setup, we need a motor with power rating of 45 kW (60 H. P.) motor with armature supply: 400 V, armature current: 90 A, field supply: 200 V, field current: 5 A. In this project, a test set up has been developed for concept testing, using a 0.746 kW (1 H. P.) separately excited dc motor. With this motor, the setup can be used for dissipating approximately 2.9 kJ energy in 4 s in the brake under test.

Development of simulated moment of inertia system was carried out in three stages: hardware development, software development, and integration and testing. In hardware development, each component was individually tested. Integration involved integration of hardware and software to develop the complete test system. Finally the test setup was used for testing of brakes.

3.3 Hardware development

Hardware development involved development of mechanical model of inertia device, speed measurement, frequency-to-voltage converter, current sensing for torque

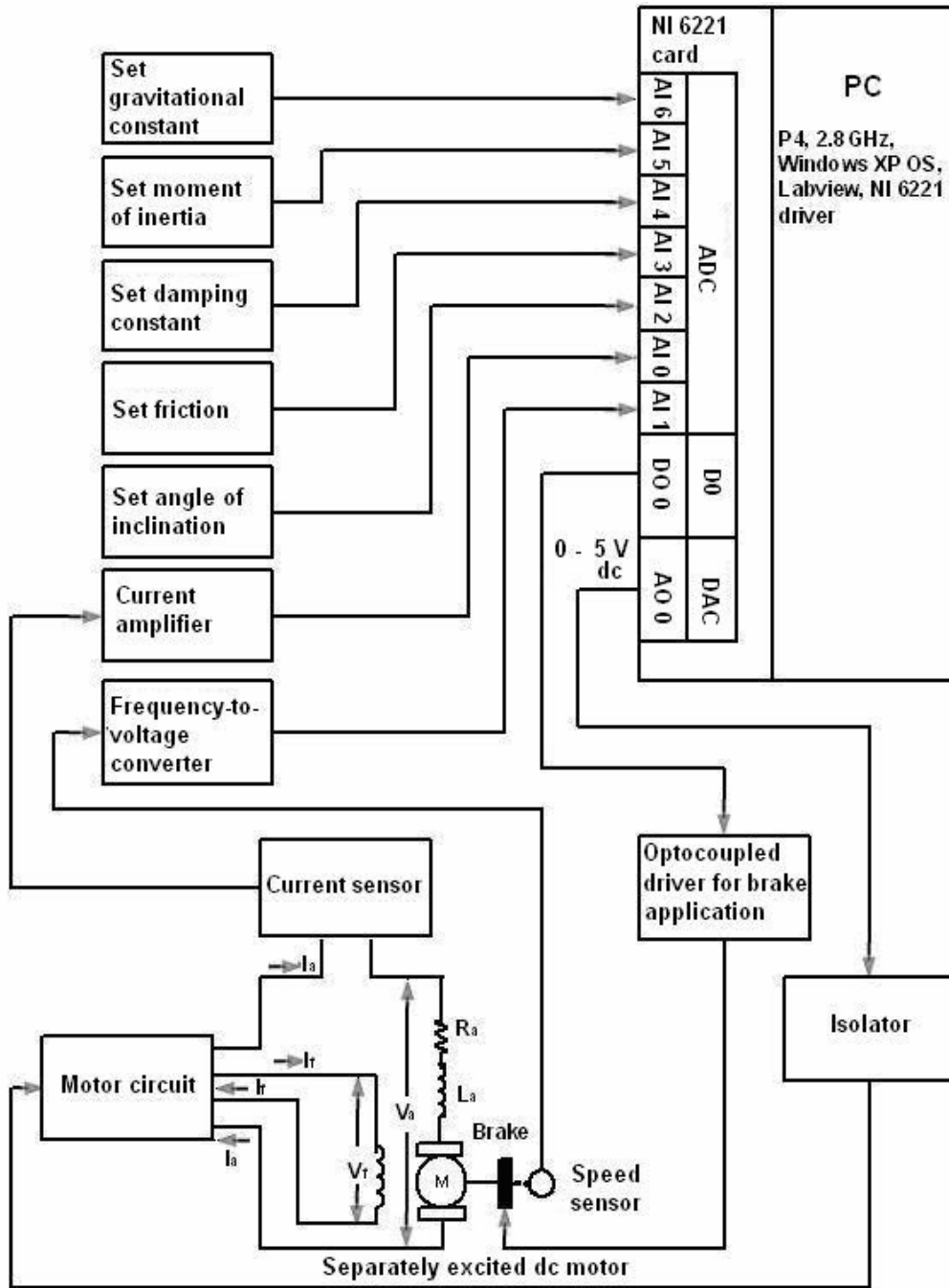


Fig. 3.1 Block diagram of the proposed electronically controlled setup.

3.3.1 Separately excited dc motor

In separately excited dc motor, field and armature voltages can be controlled independently as shown in Fig. 3.2. If the conversion is from mechanical to electrical, the separately excited dc motor is said to act as a generator. The brake mode is a generator action by which electrical power generated is either regenerated or dissipated within the motor that develops a mechanical braking effect [25] - [28]. If the conversion is from electrical to mechanical, the separately excited dc motor is said to act as a motor [29] - [31]. Therefore, the same separately excited dc motor can be made to operate as a generator or as a motor. The major advantages of separately excited dc motor are easy speed and torque regulation. During speed control application, speed of the motor is measured with an incremental encoder or magnetic pulse pick up [32] - [35]. In case of separately excited dc motor, torque is directly proportional to armature current [26]. In an application, the motor is used for providing mechanical torque, as the driving engine before the brake application, and sum of inertial, damping and friction torque after the application of the brake. “Librathern” model 2K6 a separately excited 0.746 kW (1 H. P.) motor, (photograph shown in Fig. 3.3), has been used in the setup. Specifications of this motor are given in Table 3.1.

Table 3.1 Specifications of 746 W separately excited dc motor used in test setup.

| | |
|------------------|--------------------|
| Manufacturer | Librathern |
| Model number | 2K6 |
| Power | 0.746 kW (1 H. P.) |
| Speed | 1500 rev./min. |
| Armature voltage | 200 V |
| Armature current | 4 A |
| Field voltage | 200 V |

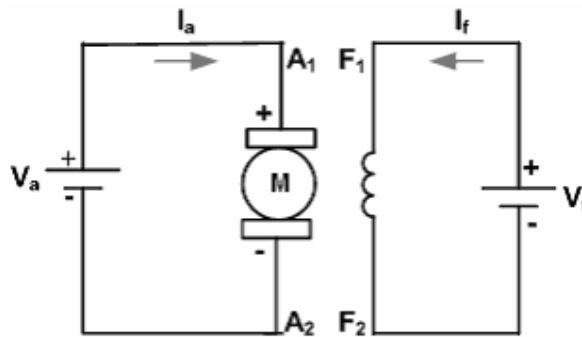


Fig. 3.2 Separately excited dc motor diagram [26].

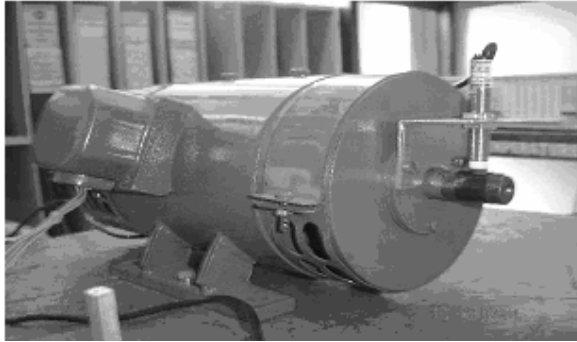


Fig. 3.3 Photograph of separately excited dc motor used in the setup: make “Librathern” model 2K6, 0.746 kW (1 H. P.).

3.3.2 Speed measurement

For speed measurement, a magnetic pulse pickup is used. A 60 toothed wheel is mounted on the motor shaft. Magnetic pulse pickup is mounted on mounting plate in such a fashion that distance between the tip of the magnetic pulse pick up and tooth of the wheel is 1 mm. The assembly is shown in Fig. 3.5. The sensor is connected to a frequency-to-voltage converter whose output is given to the data acquisition card NI 6221. It may be noted that the magnetic pulse pickup output could have been directly inputted to the data acquisition card. External frequency-to-voltage converter has permitted a simpler software interface for all the inputs of Fig. 3.1

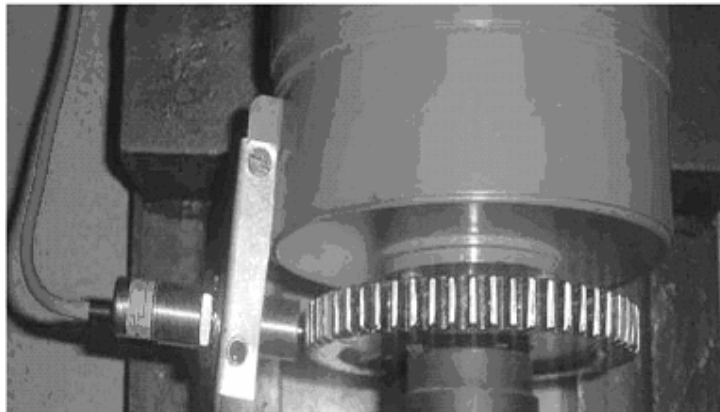


Fig. 3.4 Photograph of speed measurement arrangement.

Block diagram of the frequency-to-voltage converter is shown in Fig. 3.5. It uses IC XR 4151 for frequency-to-voltage conversion. The frequency-to-voltage converter

consists of inbuilt power supply of 15 V dc to give supply to magnetic pulse pickup, wave shaping circuit, and IC XR 4151 and its related circuit. Output of magnetic pulse pickup is a square wave with amplitude of 0 to 15 V dc. Frequency-to-voltage converter converts the frequency signal to voltage signal. Response time is 500 μ s. The circuit was tested for 0 - 1500 Hz input frequency, and the output voltage was found to vary linearly over 0 - 10 V dc.

Speed sensed by the magnetic pulse pickup is displayed by the software. Over the range of 0 - 1500 rev. /min, difference between speed reading on computer and speed measurement using a stroboscope was within ± 1 rev. /min.

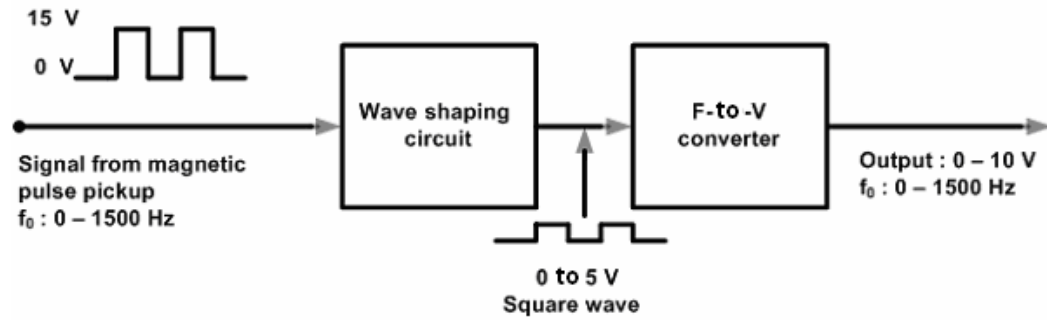


Fig. 3.5 Block diagram of frequency-to-voltage converter [Librathern, model ISM10]

3.3.3 Current sensing for torque measurement

In a separately excited dc motor with constant field flux, torque is proportional to armature current. Hence the torque can be calculated by sensing armature current, by measuring the voltage drop across a small resistor connected in series with armature winding.

The armature current, which is sensed by connecting a Shunt (5 A dc, 75 mV) in series with the armature of the motor. The Shunt voltage is amplified to provide 0 to 10 V dc corresponding to 0 to 75 mV, and after optical isolation, this signal is given to the input of data acquisition card NI 6221. The current signal was verified by connecting a dc current meter in series with the armature.

For a separately excited dc motor, the torque T in Nm for current I_a in A can be calculated as

$$T = c_1 I_a \quad (3.8)$$

For the 0.746 kW motor used, the maximum torque is T_m 6.8 Nm for $I_a = 4$ A, and hence the torque to armature current ratio c_1 calculated from (3.8) is 1.7 Nm /A.

3.3.4 Development of the mechanical test setup

Separately excited dc motor is mounted on a base. For speed measurement, speed sensor is mounted on the fixed part of the motor and the toothed wheel is mounted on the shaft of the separately excited dc motor. Earthing point is connected to earth terminal of the supply, for reducing the electrical noise problem during the test. Brake is mounted on the motor shaft as shown in Fig. 3.6. Inertia device prototype is shown in Fig. 3.7.

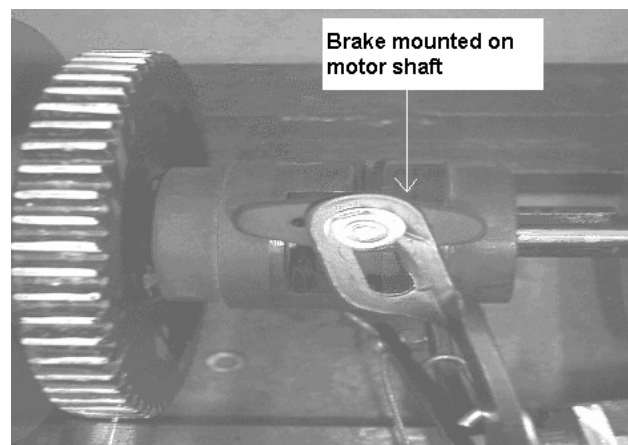


Fig. 3.6 Photograph of brake fixing on the motor shaft.

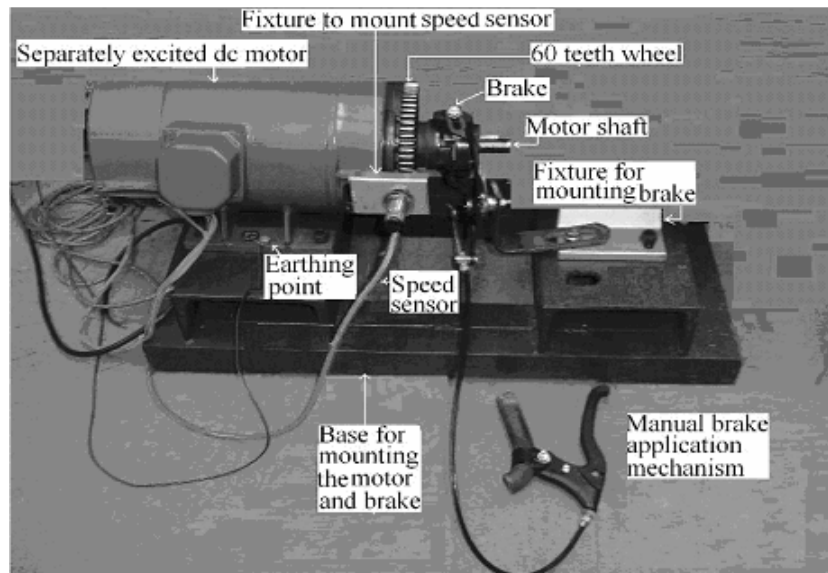


Fig. 3.7 Photograph of mechanical setup of test system.

3.3.5 Drive for armature controlled separately excited dc motor

Libratherm make semi-converter dc drive is used for controlling motor speed. It consists of two bridges. A fixed 200 V dc voltage supply is given to field winding through rectifier bridge. Armature winding is connected to semi-converter bridge. Motor speed is controlled by varying the armature voltage over 0 - 200 V dc by controlling the thyristor firing angle by giving control voltage 0 - 5 V dc externally. Wiring diagram of drive is shown in Fig. 3.8.

Features of the drive are: soft start, soft stop, maximum speed set, minimum speed set, field failure detection, current limit set, and current trip. The speed is governed by the armature voltage and the load on the motor shaft. Drive permits continuous variation of the firing angle to provide continuous linear variable output to vary in accordance with the input, presettable linear acceleration and deceleration for soft start and soft stop, over load protection and provides a normally open contact which can be used for visual indication or audible output, electronic current limit and fuse protection to protect the motor winding from overload current. A relationship between input control voltage, drive output and speed of the motor are shown in Table 3.2.

Immediate application of full voltage to the motor armature results in very high inrush current. The soft start feature allows the output to build over a period of 0 to 15 s and eliminates any possibility of high current surges. Current limit is adjustable from 50 % to 150 % of the rated current. Loading on the motor more than its capacity will heat the windings of the motor and the motor may get damaged. The current limit action circuitry limits the output current and protects the motor from getting damaged.

Table 3.2 Input control voltages, observed voltage across dc drive and motor speed relationship.

| Input control signal (V) | Observed voltage across dc drive (V) | Motor speed (rev./min.) without any load |
|--------------------------|--------------------------------------|--|
| 0.0 | 0 | 0 |
| 1.0 | 43 | 250 |
| 2.0 | 84 | 560 |
| 3.0 | 125 | 880 |
| 4.0 | 165 | 1190 |
| 5.0 | 200 | 1500 |

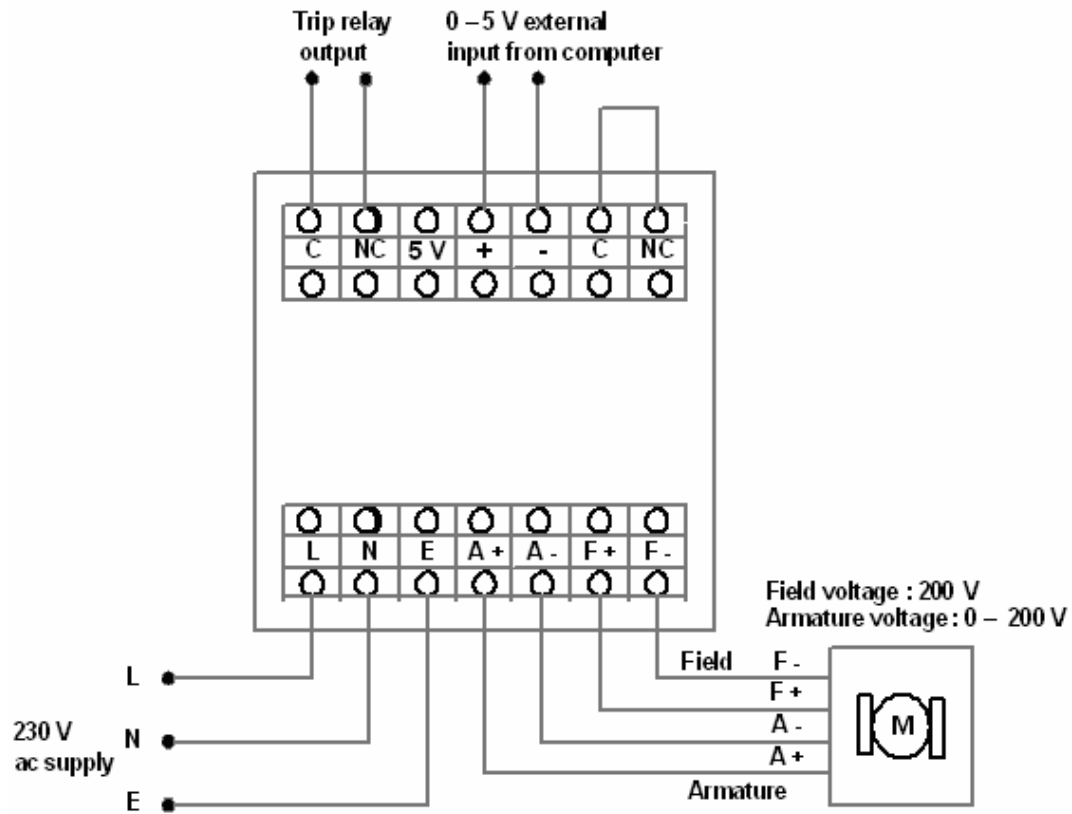


Fig. 3.8 Wiring diagram of drive of make Libratherm, model TDM - 1000.

3.3.6 Isolator unit

Isolator unit is used to electrically isolate the analog output of the data acquisition card from the dc drive circuit. The block diagram of the isolator is shown in Fig. 3.9. It consists of voltage-to-frequency converter, Optoisolator, and frequency-to-voltage converter. Voltage signal is applied to the input of the isolator. Voltage-to-frequency converter converts input voltage to frequency signal by using IC XR4151. Signal is optically isolated using optoisolator IC MCT 2E. Its signal conversion time is 5 μ s. The optically isolated signal is given to frequency-to-voltage converter block. It converts the frequency signal to voltage signal using IC XR4151. Thus input analog signal is optically isolated from the output analog signal. When input voltage given to the isolator unit is switched from 0 to 5 V dc, the response time of the isolator is 80 ms. For testing the isolator, voltages in the range of 0 - 5 V dc were given as input to the isolator with the help of a standard calibrator and corresponding output voltages of the isolator

unit were recorded on a digital oscilloscope. The input and output voltage relation along with the response time for step change in the input is given in Table 3.3.

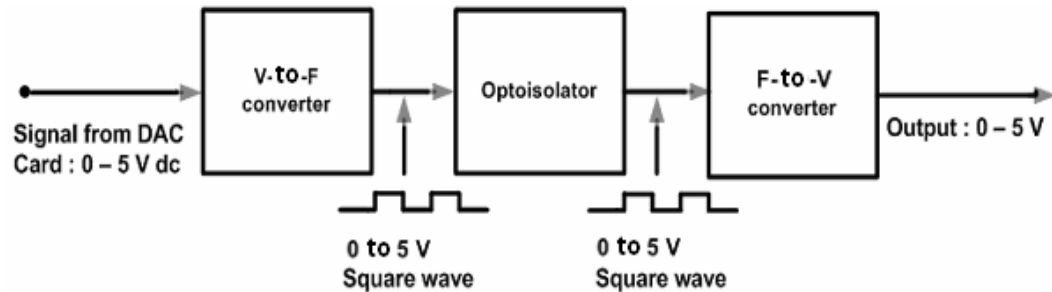


Fig. 3.9 Block diagram of isolator of make Libratherm, model ISM - 10.

Table 3.3 Relationship between input voltage and output voltage of the analog optoisolator

| Input (V) | Output (V) | Response time for step input (ms) |
|-----------|------------|-----------------------------------|
| 0.000 | 0.000 | 0 |
| 1.000 | 1.001 | 15 |
| 2.000 | 2.003 | 30 |
| 3.000 | 3.001 | 45 |
| 4.000 | 4.002 | 60 |
| 5.000 | 5.001 | 80 |

3.3.7 Solenoid for application of the brake

A 12 V dc solenoid is used to control the application of the brake. Digital output P0.0 from NI 6221 is connected to optoisolator as shown in Fig. 3.10. When digital output P0.0 becomes high, it drives the optoisolator. Optoisolator drives the 24 V dc relay RLY1. Normally open contact (RLY1 A) of relay RLY1 becomes closed and 230 V ac supply is given to contactor RLY2 which operates on 230 V ac supply. A normally open contact (RLY2 A, B, and C) of relay RLY2 becomes closed and 12 V dc supply is given to solenoid coil and brake gets applied.

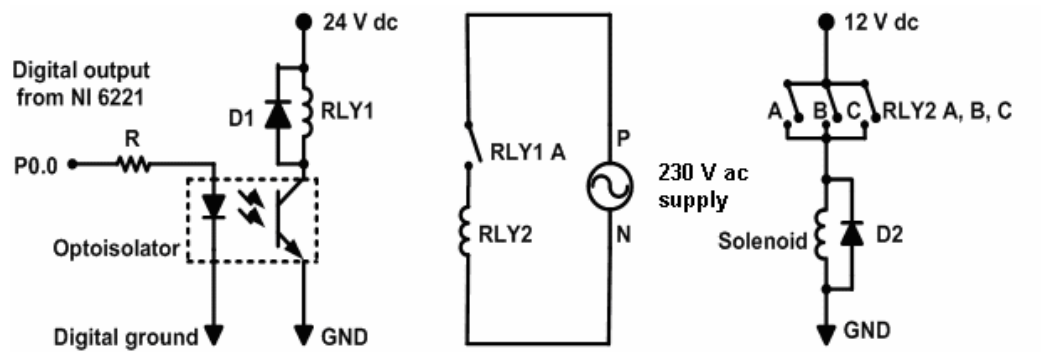


Fig. 3.10 Solenoid driver circuit developed.

3.3.8 Industrial computer

At the core of the setup is an industrial PC, IPC - 611 from M/s Dynalog as shown in Fig. 3.11. It has Intel P4 processor with 2.8 GHz clock, 512 MB dual data RAM, 40 GB HDD, 4 PCI slots, 250 W supply, keyboard, mouse and monitor, and Windows XP operating system. One of the PCI slots is used for data acquisition card NI 6221.



Fig. 3.11 Photograph of industrial computer of make Dynalog, model IPC - 611.

3.3.9 Data acquisition card

Data acquisition card NI 6221, from National Instruments, is used to interface the field signals with software. The card is fitted in one of the PCI slots of the industrial computer. It has 16 analog inputs, two analog outputs, ten digital input lines and ten digital output lines. Pin connections of data acquisition card are given in Appendix A. NI 6221 card driver software is installed to interface the card with the Labview package. With the help of NI 6221 card driver software, it is possible to check the

operation of the card. Shielded cables are used to terminate the analog and digital input and output signals on terminal box as shown in Fig. 3.12. All 16 analog inputs were calibrated by sourcing 0 to 10 V dc signal from a standard calibrator. Two analog outputs were checked by monitoring the 0 to 10 V dc signal on a DSO. Digital input and output were checked by programming each digital line as input or output line through NI 6221 card driver software. When digital line is programmed as digital output; voltage level measured on that digital line should be + 5 V dc. When digital line is programmed as digital input, + 5 V dc signal given to that digital line is taken as digital input 1 and 0 V dc as digital input 0. Software panel used to check all analog and digital input / output signals of the card are shown in Appendix B.

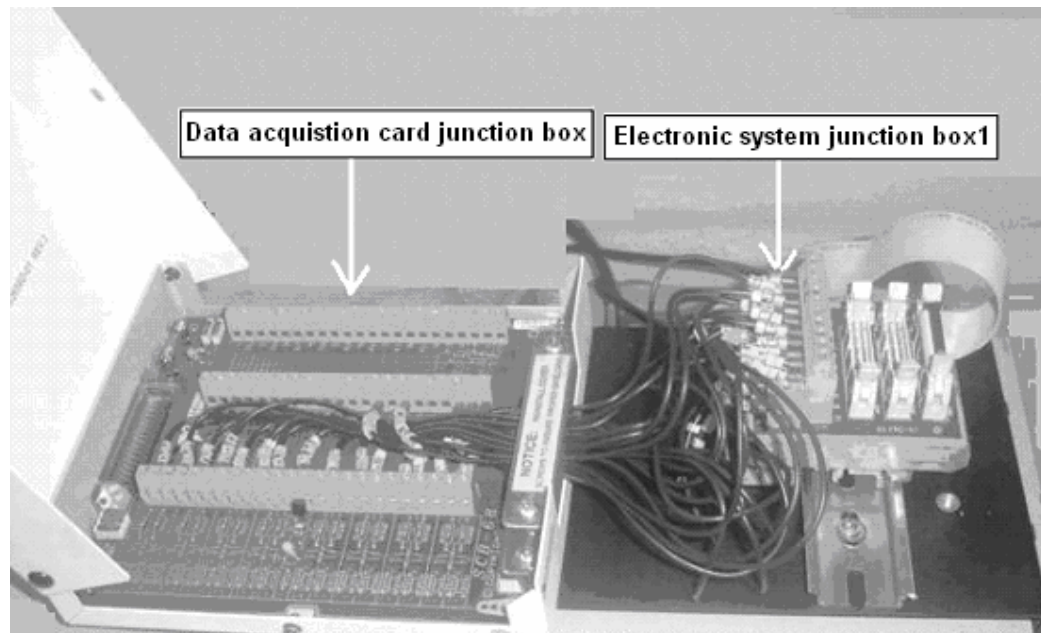


Fig. 3.12 Photograph of terminal block to interface data acquisition card NI 6221 with electronic system junction box1.

3.4 Software development

Software development involved development of graphical user interface panels, configuration of channels, and development of control system algorithm, graphical representation of speed and torque along with time, data acquisition of test data, alarm configuration for safety of device and test components.

Logic and graphical user interface were developed in Labview package from National Instruments. Labview package is an open environment for interfacing PC with

measurement hardware, with interactive assistance for code generation. It has about 500 built-in functions designed for extracting information of the acquired data and for analyzing measurements and processing signals. It provides tools for user interface design, report generation, data management, software connectivity, and control. In structured software engineering processes, software development begins with establishing system and software requirements and continues with architectural design, code testing, and debugging. First phase of software development is fixing the components for building the system, including the hardware requirements, software tools, performance requirements, and user interface requirements. Second phase is design, which determines the software framework of a system to meet the specified requirements. It defines the system components and their interaction, and the external interfaces and tools. Third phase of development implements the design specification in code. Debugging tools in Labview package include execution highlight, which shows the movement of data on the block diagram from one node to another using bubbles that move along the wires. Single stepping, which steps through a program, shows each action of the program on the block diagram as the program runs. Breakpoints can be placed on a program, node, or wire on the block diagram to pause execution at that location. Testing determines whether the software meets the specified requirements and finds any errors present in the code.

3.4.1 Graphical user interface (GUI) development for test system

Various graphic interfaces are developed in menu format. There are the following menus: configuration menu, main menu, system menu, and alarm menu, as shown in Appendix C. Configuration menu configures voltage levels of analog input channel. Main menu is main screen of software which controls the program. Alarm menu is used to set the alarm for safety of the system and the component to be tested. System menu sets the control parameters of the test system.

3.4.2 Main menu

In main menu, the parameters shown are sensed torque in Nm, sensed speed in rev./min., sensed angular speed in rad/s, set value of inertia constant, damping constant, friction constant, speed, brake delay time, maximum brake application time, numbers of cycles, energy to be dissipated in brake. Torque and speed parameters are shown online

with respect to time in graphical format. There is start and stop button to start the system and to stop the system. When the start button is pressed, the main menu function executes until stop switch is activated. When any alarm or stop button is activated, the program comes out from the main menu and stops the test.

3.4.3 Channel configuration menu

Configuration menu configures maximum and minimum voltage levels of analog input channels. All analog signals represent an input variable with a linear relationship.

$$y = mx \quad (3.9)$$

where x is the analog input and y is the corresponding physical parameter. Based on (3.1), (3.2), (3.3), (3.4), (3.5), and (3.9), the seven input channels along with their slopes, voltage range, and signal range are listed in Table 3.4. Two-point calibration is carried out for each channel, by sourcing maximum and minimum voltage using a standard voltage calibrator.

Table 3.4 List of sensed and set parameters, input through ADC channels.

| Input | | | | Voltage Input | | | Slope | |
|--------------------------|----------|------------|-------------------|----------------|------------|----------------|------------|--------|
| Parameter | Sym-bol | Max. value | Unit | Analog channel | Sym-bol | Max. value (V) | Sym-bol | Slope |
| Sensed torque | T | 6.80 | Nm | AI 0 | V_T | 8.00 | m_T | 0.85 |
| Sensed speed | N | 1500 | rev./min. | AI 1 | V_N | 10.00 | m_N | 150 |
| Set angle of inclination | α | $\pi / 4$ | rad | AI 2 | V_α | 10.00 | m_α | 0.079 |
| Set friction constant | T_f | 0.50 | Nm | AI 3 | V_{Tf} | 10.00 | m_{Tf} | 0.05 |
| Set damping constant | b | 0.003 | (Nm s)/rad | AI 4 | V_b | 10.00 | m_b | 0.0003 |
| Set moment of inertia | J | 0.45 | kg m ² | AI 5 | V_J | 10.00 | m_J | 0.045 |
| Set gravitational torque | T_{gm} | 6.80 | Nm | AI 6 | V_{gm} | 10.00 | m_{gm} | 0.68 |

3.4.4 Alarm menu

Alarm screen has three settings: alarm setting, alarm indicators and alarm actions. Alarm actions decide whether to continue the testing or stop the testing. Values in alarm setting are compared with the actual values of respective channels. If actual value is more than set value, alarm occurs and testing gets stopped or continues depending on alarm action condition set during starting of the testing.

3.4.5 System menu

All test system control parameters can be set in the system menu. Speed demand limiter and the sampling rate are set through this menu. Before starting the test, system prompts for file name to store the data. The data are stored in binary format. For attaining the set speed before brake application we can either use close loop control (with speed feedback as process variable for speed control and current feedback as process variable for torque control) or open loop control.

3.5 Inertia logic development

An inertia dynamometer setup for brake testing, as shown in Fig 2.7, consists of electric motor coupled with transmission unit where the brakes are fitted. Flywheel is coupled to the motor shaft. Flywheel is selected based on energy to be stored before application of the brake. The test system follows the following sequence. With brake in released condition, electric motor speed is increased to drive shaft speed. When motor reaches the drive shaft speed, the control system removes the signal to the drive. The rear axles and drive shaft rotate due to inertial energy stored in the flywheel. Brakes are applied on the rear wheels. The kinetic energy of the rotating flywheel is dissipated by the brake. When rear axle speed becomes zero, brakes are released and same cycle is repeated for a predefined number of cycles for endurance test. With the help of this test setup it is possible to conduct endurance, performance, and burnishing tests.

Electronically controlled inertia system consists of separately excited dc motor with control software. In this system, the brakes are applied after the set speed is reached. The motor continues providing torque during the braking action. The drive circuit of the motor is controlled in such a way that torque provided by the motor is sum of the torques due to moment of inertia, damping, friction etc, for the instantaneous

speed and deceleration. Alarm of the respective channels is set with the help of alarm screen. Each alarm has two actions, which are “stop test” and “continue test”. If stop option is selected, the test will stop after activation of alarm. If continue option is selected, the test will continue after activation of alarm. Deceleration time is the time in which motor will come to zero speed, is also set.

The control system operates as follows. Set the sampling rate and start the test system by clicking on the “Start” button on the main menu. The values set for inertia, damping, friction, angle of inclination, gravitational constant are continuously read from the input channels and displayed. These values can be adjusted by corresponding potentiometers. The value of set speed, wait time before brake application, maximum brake application time, set energy value, set number of cycles, instantaneous speed demand value are set through the menu. The alarm value like inertia, damping, and friction, angle of inclination, gravitational constant, speed, and torque are set through the alarm menu. For reading the set speed before brake application we can either use close loop control (with speed feedback as process variable for speed control and current feedback as process variable for torque control) or open loop control through system menu. After setting all the test values, “Ok” button be clicked. The motor drive is given the control signal to achieve the set speed. After set speed is achieved, brakes are applied after the set wait duration. After brake application, the software calculates the power and energy dissipated in brake from speed and torque reading for every sampling instance and adjusts the required torque by varying the drive current to the motor. Thus control system dissipates the required energy by controlling the angular velocity. When dissipated energy in brake is equal to set energy, the brake is released. In case set energy cannot be dissipated in brake and the set time elapses, the brake is released. This is an indication of poor performance of the brake. Test cycles are repeated for a preset quantity.

3.6 Development of control system

Block diagram showing connections between instruments and inertia device is shown earlier in Fig. 3.1. System is divided in two parts, one part is PC based hardware and other part is control circuit with inertia device

At no load (brake in the released condition) and constant speed, the torque acting on motor shaft is torque due to kinetic friction and damping torque. Motor voltage is increased to maintain the speed by overcoming the friction and damping. Let the no load speed of the motor be N_m for voltage V_{sm} supplied to drive voltage. We define control voltage to speed ratio as

$$K_1 = V_{sm} / N_m \quad (3.10)$$

and use it to generate the control voltage for desired change ΔN_s as

$$V_s = K_1 \Delta N_s \quad (3.11)$$

For rated armature voltage, let the maximum torque be T_m and the maximum speed be N_m , we define speed-to-torque ratio as

$$K_2 = N_m / T_m \quad (3.12)$$

This ratio is used for generating a required torque T as a speed demand N as

$$N = K_2 T \quad (3.13)$$

which is converted into control voltage used (3.11).

Table 3.5 Test system parameter

| Symbol | Description | Value | Unit |
|----------------------|---|--------|------------------|
| N_m | Maximum speed | 1500 | rev. / min. |
| V_{sm} | Maximum control voltage supplied to drive | 5.00 | V |
| T_m | Maximum torque | 6.80 | Nm |
| $K_1 = V_{sm} / N_m$ | Voltage to speed ratio | 0.01 | V min. / rev. |
| $K_2 = N_m / T_m$ | Speed to torque ratio | 220.60 | rev. / (min. Nm) |

3.7 Software architecture

Software is divided in three control modules: Module 1 for controlling set speed before application of brake (Fig. 3.13), Module 2 to control energy dissipated in brake (Fig. 3.14), and Module 3 to stop the test system. Execution of all the operation in each of the module is repeated at set sampling frequency $f_s (=1/\Delta t)$.

Module 1 (Fig. 3.13): Let N_s = set speed, V_T = the torque sensor output voltage corresponding to torque T , V_N = speed sensor output voltage corresponding to speed N , m_N = slope of the speed signal of the motor, m_T = slope of the torque signal. Set speed and actual speed signal feedback are given to the error detector. Output of the error detector (ΔN_s) is given to speed demand limiter block. If speed demand signal to drive coming from error detector exceeds the maximum set speed in limiter, then software adjusts the demand equal to maximum set demand limit in the limiter. Output of the demand limiter, is given to speed-to-voltage converter block, which converts the speed demand signal to voltage output. Time comparator keeps the track of the time signal by taking two time inputs which are time elapsed after starting the test system t_{es} and the set time to apply the brake t_{ab} . Time t_{es} is calculated by a software function using on-board timer of DAQ. When t_{es} become equal to t_{ab} , software enters into “Module 2”. In Module 1, speed and torque signals are recorded in the file. Speed and torque signals are given to alarm system. If any alarm occurs, the software stops the test rig.

Module 2 (Fig. 3.14): Let V_J = voltage corresponds to moment of inertia J , V_b = voltage corresponds to damping constant b , V_{Tf} = voltage corresponds to friction constant T_f , V_{gm} = voltage corresponds to gravitational constant. Let m_J , m_d , m_{Tf} , m_{gm} be their slopes respectively. From these parameters angular velocity ω , deceleration, power P , energy E are calculated. Control unit compares the set energy E_s with the actual energy dissipated in brake after application of the brake. It calculates total set torque T_s due to moment of inertia, damping, friction, gravitational constant, and angle of inclination. Speed-to-torque ratio K_2 is used to calculate the speed demand signal from T_s . Speed demand signal is given to speed to voltage converter block through demand limiter block which converts the speed demand signal to voltage output. Time comparator keeps track of the time signal by taking two time inputs: (i) maximum brake application time, t_b , and (ii) time elapsed after application of brake, t_{eb} . When $t_{eb} \geq t_b$, counter gets incremented and control goes to Module 1. If set number of cycles are

completed then the test rig stops. In Module 2, speed signal, torque signal, angular velocity signal, power, energy, and deceleration are recorded in the file. Speed and torque signals are given to alarm system.

Module 3: The program enters Module3 if any alarm condition is met. Zero speed demand is given to the drive circuit to stop the motor and the over all system operation is stopped.

After initialization, Module1, Module2, Module3 are executed for every time interval Δt based on set sampling frequency f_s ($=1/\Delta t$). The main program algorithm may be described as follows.

1. Initialization

- 1.1 Set the sampling frequency f_s to a value between 5 Hz to 150 Hz from the main menu.
- 1.2 Set the maximum speed of the motor from main menu.
- 1.3 Set the moment of inertia from A/D channel.
- 1.4 Set the damping coefficient from A/D channel.
- 1.5 Set the friction force from A/D channel.
- 1.6 Set the maximum stopping time from main menu.
- 1.7 Set the time after which brake is applied from main menu.
- 1.8 Set net energy to be dissipated in brake from main menu.
- 1.9 Set number of cycles for test to be carried out from main menu.
- 1.10 Activate alarm for speed and torque for safety purpose from alarm menu.
- 1.11 Set data recording rate, text file name, and its storage location on hard disk from main menu.

2. Wait for start button on main menu screen to start the system by activating Module 1

3. Module 1:

- 3.1 Brake is in released condition.
- 3.2 Initialize the timer and energy storage variable before application of brake.
- 3.3 Start data recording.
- 3.4 Speed demand is given to dc drive to reach set speed.
- 3.5 If any alarm is activated, go to step 5

- 3.6 If set speed is not achieved then, retain control in Module 1 by going to step 3.4 after the set sampling interval ($1/f_s$)
- 3.7 If system timer is equal to brake application delay timer, go to Module 2

4. Module 2:

- 4.1 Give control for brake application.
- 4.2 Start brake application timer.
- 4.3 Calculate the angular velocity.
- 4.4 Calculate the deceleration by taking derivative of the angular velocity.
- 4.5 Calculate the power from speed and torque values.
- 4.6 Calculate the torque due to inertia from deceleration and inertia constant, torque due to damping force from angular velocity and, torque due to friction, and torque due to gravitation.
- 4.7 Calculate the net torque by adding torque due to inertia, torque due to damping, torque due to friction, and torque due to gravitation.
- 4.8 From the set torque, calculate the set speed from speed-to-torque ratio parameter of test system.
- 4.9 Calculate the energy dissipated in brake from the power and time values for every instance of time and add the energy value in variable where energy dissipated values gets added for every instance of time after application of brake.
- 4.10 If any alarm is activated, go to Module 3.
- 4.11 If braking time becomes equal to maximum braking time, release brake, increment cycle counter and give control to step 4.13.
- 4.12 If energy dissipated in brake is equal to set energy to be dissipated, release brake, increment cycle counter and give control to step 4.13.
- 4.13 If number of cycles equal to set number of cycles in counter, go to Module3
- 4.14 Go to Module 1

5. Module 3

- 5.1 Stop data recording.
- 5.2 Release the brake.
- 5.3 Set speed demand to zero and stop the motor.
- 5.4 Stop the program.

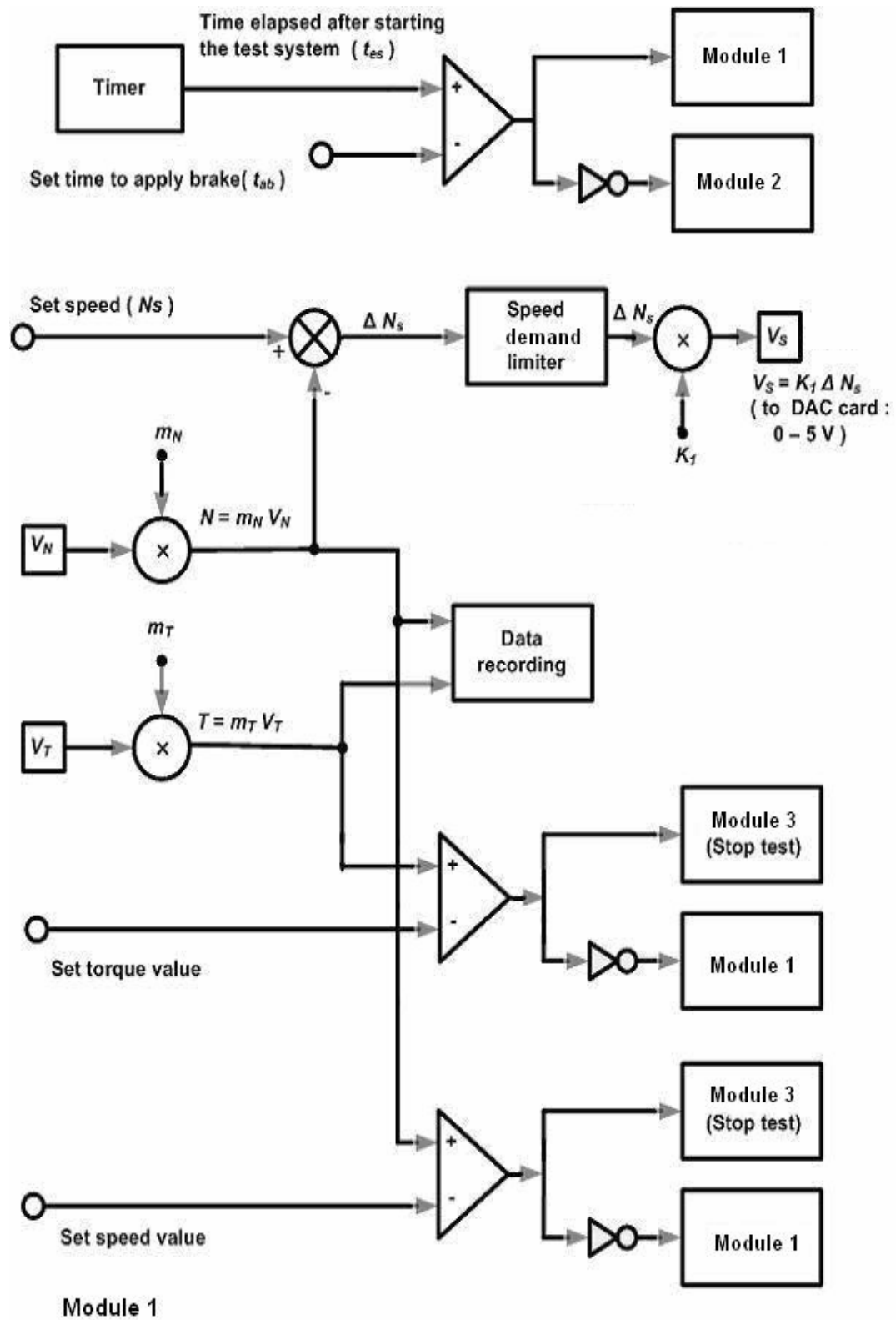


Fig. 3.13 Module 1 for controlling set speed before application of brake.

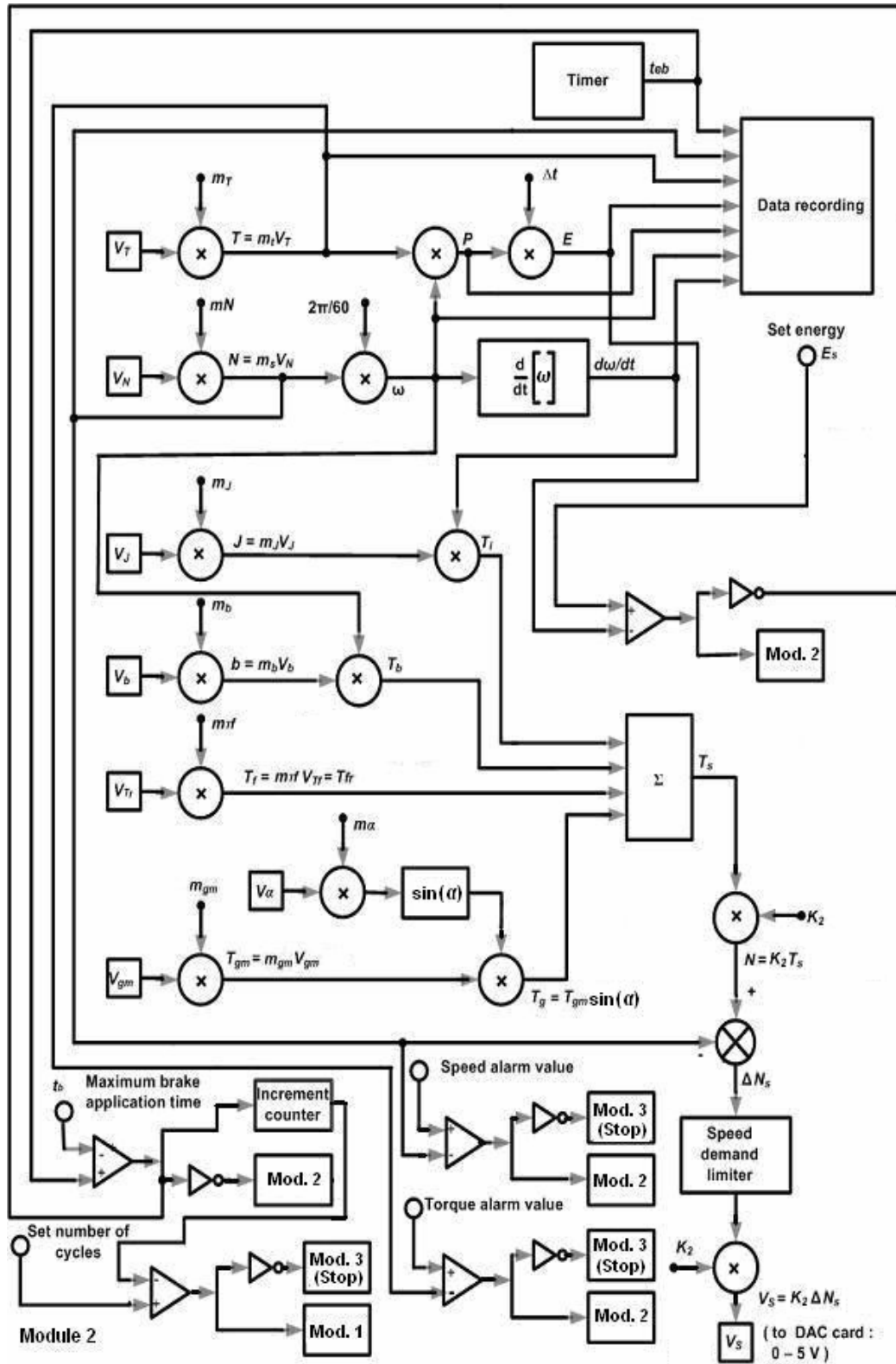


Fig. 3.14 Module 2 for controlling energy dissipated in brake.

3.8 Integration and debugging

All hardware and software has been checked independently. System has been developed by integrating all hardware modules like speed and current sensors, signal amplifier, presetting of damping, inertia, friction constants, NI 6221 data acquisition card interfacing, installation of industrial computer, loading of Labview package, installation of the NI 6221 card, termination of the all analog and digital input and output signals on the terminal box. NI 6221 data acquisition card driver software was installed on the computer. Checking of all analog and digital input and output signals in software.

Values of damping force, deceleration time, acceleration time, angular velocity, inertia constant, friction constant are set through potentiometers. Constant 10 V dc supply is given to the potentiometer from a 10 V dc power supply. Speed and current signals are given to analog input channels of the data acquisition card. One digital output is used to drive the solenoid which is used to apply brakes. Speed sensor output is used to drive the solenoid which is used to apply brakes. Speed sensor output is given to frequency-to-voltage converter to convert the speed signal to voltage. Speed signal is used as feedback signal to control the speed. Shunt (5 A dc, 75 mV dc) is used to measure the current in the armature circuit. Voltage across resistor is amplified with the help of voltage amplifier. As the motor is separately excited dc motor, so torque of the motor is directly proportional to current. List of modules and components required for test system are listed in Appendix C.

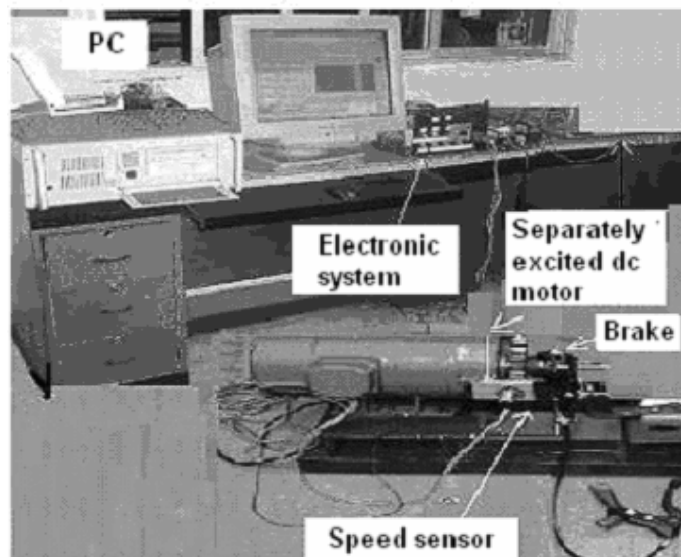


Fig. 3.15 Photograph of test setup developed.

Test setup developed is shown in Fig. 3.15. Electronic system developed for test system is shown in Fig. 3.16. Safety interlock is given by a contactor to shutdown the system in case of emergency. When power is given to drive, control circuit, and computer, the contactor gets on and connects the armature winding of the motor to the drive. If the power fails, the contactor gets switched off and disconnects the armature supply of the motor. In alarm condition or power failure condition, brake is in released condition. During test if power fails or any test alarm occurs, supply given to the solenoid is removed to release the brake.

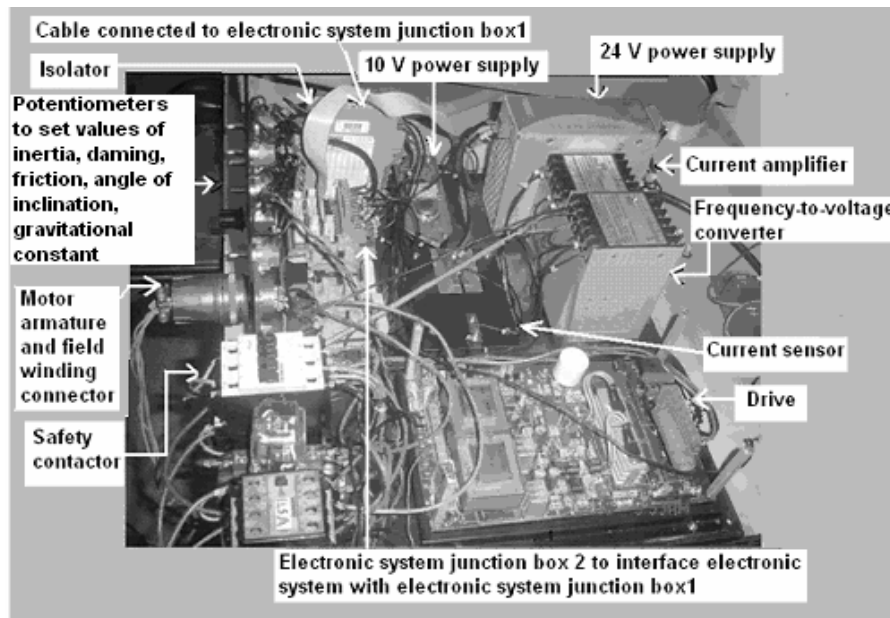


Fig. 3.16 Photograph of electronic system developed for test system

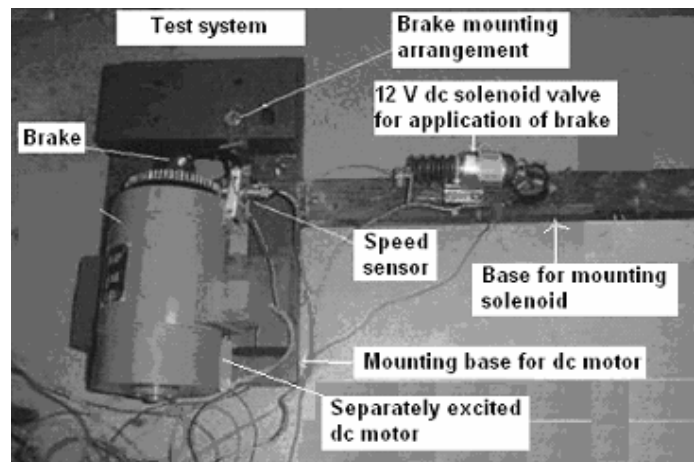


Fig. 3.17 Photograph of test setup developed for endurance testing of brake

Endurance testing of brake test setup is shown in Fig 3.17. In this setup brake is applied through another 12 V dc solenoid. Two timers are programmed in software. One timer is “Off timer” and other is “On timer”. When “Off timer” is activated the brake is in released condition. When “On timer” is activated, the brake gets applied for that time period. When the brake has been applied the set energy is not dissipated within on-time period of the “On timer”, because of the insufficient brake force or a slippery brake, the program will release the brake and “off timer” gets started. Endurance testing of brake is carried out for a set number of cycles, with motor being stopped after each cycle. Measured parameters and calculated parameters are recorded in a text file.

3.9 Testing and qualification

In this process, complete test is carried out. Software screen optimization is carried out by properly selecting the data range as per specifications of the test system. There is an upper safe limit for user inputs for parameters like set energy, set speed etc. The software displays a message if the set values of inertia, damping constant, and friction are not properly set by the user. For proper working of test system, appropriate value of sampling frequency should be used.

3.10 Sampling frequency selection

In this setup, we do not have definite information on the bandwidth of the speed and torque signals and hence the required minimum sampling rate. If sampling rate is too low, measurements are likely to be in error because of aliasing errors. If the sampling rate becomes so high that program execution does not take place in real time, we will again have errors. For values of sampling frequency in between the lower and upper limits for usable sampling frequency, we should get valid observation. The test rig was operated with combination of different values of parameters. Each combination is labeled as a “Test” as listed in Table 3.6. Each of these tests was carried out for a set of sampling rates and the braking time was observed for each case and is tabulated in Table 3.7.

For empirically determining the acceptable range of sampling frequency, we have calculated the correlation coefficient and mean magnitude difference between observed braking time for pairs of sampling frequencies.

Correlation coefficient [36] between two set of data $\mathbf{x} \{x_1, x_2, \dots, x_n\}$ and $\mathbf{y} \{y_1, y_2, \dots, y_n\}$, with n observations and sample mean of \bar{x} and \bar{y} is given as

$$r_{xy} = \frac{\sum_{i=1}^n (x_i - \bar{x})(y_i - \bar{y})}{\sqrt{\left[\sum_{i=1}^n (x_i - \bar{x})^2 \right]} \sqrt{\left[\sum_{i=1}^n (y_i - \bar{y})^2 \right]}} \quad (3.14)$$

and it is a measure of degree of association. Correlation coefficients for pair of frequencies was calculated, taking the braking time for dissipating the set value of energy for different test conditions as observed data points and the values are given in Table 3.8. Results show a very high correlation for frequency pairs in the range of 10 Hz to 150 Hz. Thus we conclude that $150 \text{ Hz} \geq f_s \geq 10 \text{ Hz}$ leads to consistent test results.

Table 3.6 Combination of values of inertia, damping, and friction constant, angular speed in different tests

| Test No. | Inertia (kg m ²) | Angular speed (rad/s) | Set energy (J) | Friction constant | Damping constant (Nm s)/rad) |
|----------|------------------------------|-----------------------|-----------------|-------------------|------------------------------|
| 1 | 0.25 | 102.2 | 1000 | 0.00 | 0.00 |
| 2 | 0.35 | 102.2 | 1000 | 0.00 | 0.00 |
| 3 | 0.45 | 102.2 | 1000 | 0.00 | 0.00 |
| 4 | 0.45 | 74.7 | 1000 | 0.00 | 0.00 |
| 5 | 0.45 | 88.1 | 1000 | 0.00 | 0.00 |
| 6 | 0.45 | 102.6 | 1000 | 0.00 | 0.00 |
| 7 | 0.45 | 102.6 | 800 | 0.00 | 0.00 |
| 8 | 0.45 | 102.6 | 1200 | 0.00 | 0.00 |
| 9 | 0.45 | 102.6 | 1600 | 0.00 | 0.00 |
| 10 | 0.45 | 102.6 | 1000 | 0.68 | 0.00 |
| 11 | 0.45 | 102.6 | 1000 | 3.50 | 0.00 |
| 12 | 0.45 | 102.6 | 1000 | 6.50 | 0.00 |
| 13 | 0.45 | 102.6 | 1000 | 0.00 | 0.40 |
| 14 | 0.45 | 102.6 | 1000 | 0.00 | 0.20 |
| 15 | 0.45 | 102.6 | 1000 | 0.00 | 0.39 |

Table 3.7 Brake release time at different sampling frequency for tests involving a combination of values of inertia, damping, and friction constant and angular speed

| Brake release time (s) at different sampling frequency in Hz | | | | | | | | | | | |
|--|------|------|------|------|------|------|------|------|------|------|------|
| Test No. | 4 | 5 | 10 | 20 | 50 | 60 | 100 | 150 | 160 | 200 | 240 |
| 1 | 4.83 | 3.19 | 3.08 | 2.96 | 2.83 | 2.86 | 2.76 | 2.75 | 1.84 | 1.54 | 1.08 |
| 2 | 4.63 | 3.05 | 2.93 | 2.82 | 2.75 | 2.72 | 2.76 | 2.52 | 1.66 | 1.25 | 0.97 |
| 3 | 4.43 | 2.99 | 2.86 | 2.67 | 2.62 | 2.57 | 2.55 | 2.28 | 1.70 | 1.36 | 0.96 |
| 4 | 8.54 | 5.96 | 5.68 | 5.54 | 5.31 | 5.34 | 5.29 | 5.14 | 3.61 | 3.22 | 2.86 |
| 5 | 6.81 | 4.11 | 3.96 | 3.81 | 3.58 | 3.41 | 3.37 | 3.11 | 2.25 | 1.59 | 1.26 |
| 6 | 6.48 | 3.48 | 2.79 | 2.48 | 2.36 | 2.28 | 2.26 | 2.48 | 1.24 | 1.09 | 0.99 |
| 7 | 2.83 | 2.83 | 2.29 | 1.83 | 1.79 | 1.83 | 1.85 | 1.65 | 0.86 | 1.16 | 1.03 |
| 8 | 4.64 | 3.94 | 3.79 | 3.64 | 3.54 | 3.54 | 3.57 | 3.26 | 2.69 | 1.58 | 1.09 |
| 9 | 8.88 | 7.13 | 7.09 | 7.00 | 6.85 | 6.99 | 6.97 | 6.78 | 4.86 | 4.68 | 2.99 |
| 10 | 3.88 | 2.89 | 2.68 | 2.59 | 2.53 | 2.74 | 2.75 | 2.28 | 1.99 | 1.35 | 0.86 |
| 11 | 3.65 | 2.91 | 2.85 | 2.71 | 2.75 | 2.58 | 2.57 | 2.71 | 1.82 | 1.16 | 0.89 |
| 12 | 3.97 | 3.27 | 2.99 | 2.87 | 2.63 | 2.21 | 2.29 | 2.13 | 1.88 | 1.79 | 1.02 |
| 13 | 3.23 | 2.94 | 2.57 | 2.38 | 2.36 | 2.22 | 2.26 | 2.06 | 1.98 | 1.27 | 0.87 |
| 14 | 3.89 | 2.99 | 2.68 | 2.48 | 2.32 | 2.39 | 2.33 | 2.11 | 1.46 | 0.99 | 0.78 |
| 15 | 4.13 | 3.08 | 2.82 | 2.56 | 2.51 | 2.52 | 2.54 | 2.27 | 1.57 | 1.17 | 0.87 |

Table 3.8 Correlation coefficients between sampling frequency pairs, for braking time, for the test condition listed in Table 3.6

| Correlation coefficients matrix | | | | | | | | | | | |
|---------------------------------|-----|----------------|-------|-------|-------|-------|-------|-------|-------|-------|-------|
| | | Frequency (Hz) | | | | | | | | | |
| | | 5 | 10 | 20 | 50 | 60 | 100 | 150 | 160 | 200 | 240 |
| Frequency (Hz) | 4 | 0.907 | 0.888 | 0.883 | 0.87 | 0.862 | 0.854 | 0.879 | 0.782 | 0.804 | 0.867 |
| | 5 | | 0.991 | 0.983 | 0.979 | 0.973 | 0.973 | 0.978 | 0.936 | 0.960 | 0.969 |
| | 10 | | | 0.998 | 0.996 | 0.990 | 0.990 | 0.989 | 0.962 | 0.965 | 0.957 |
| | 20 | | | | 0.999 | 0.991 | 0.991 | 0.989 | 0.972 | 0.962 | 0.946 |
| | 50 | | | | | 0.994 | 0.995 | 0.993 | 0.976 | 0.963 | 0.944 |
| | 60 | | | | | | 0.999 | 0.993 | 0.970 | 0.957 | 0.942 |
| | 100 | | | | | | | 0.992 | 0.974 | 0.959 | 0.941 |
| | 150 | | | | | | | | 0.960 | 0.957 | 0.948 |
| | 160 | | | | | | | | | 0.945 | 0.894 |
| | 200 | | | | | | | | | | 0.955 |

The mean of the magnitude of the differences is calculated as

$$\varepsilon = \frac{1}{n} \sum_{i=1}^n |x_i - y_i| \quad (3.15)$$

Mean of the magnitude of the differences between sampling frequency pairs, for braking time, for the test condition listed in Table 3.6 are tabulated in Table 3.9. We see that this is more sensitive test for agreement before the values. The errors are lowest for pair of frequencies selected in the $50 \leq f_s \leq 100$ Hz range. Hence we may conclude that we should use sampling frequency value in this range.

Table 3.9 The mean of magnitude of differences between sampling frequency pairs, for braking time, for the test condition listed in Table 3.6

| The mean of magnitude of differences | | | | | | | | | | | |
|--------------------------------------|-----|----------------|-------|-------|-------|-------|-------|-------|-------|-------|-------|
| | | Frequency (Hz) | | | | | | | | | |
| | | 5 | 10 | 20 | 50 | 60 | 100 | 150 | 160 | 200 | 240 |
| Frequency (Hz) | 4 | 1.336 | 1.585 | 1.763 | 1.872 | 1.907 | 1.914 | 2.084 | 2.894 | 3.309 | 3.755 |
| | 5 | | 0.249 | 0.430 | 0.536 | 0.571 | 0.578 | 0.748 | 1.560 | 1.970 | 2.419 |
| | 10 | | | 0.180 | 0.286 | 0.322 | 0.329 | 0.499 | 1.310 | 1.720 | 2.170 |
| | 20 | | | | 0.108 | 0.143 | 0.151 | 0.321 | 1.130 | 1.550 | 1.992 |
| | 50 | | | | | 0.035 | 0.043 | 0.213 | 1.020 | 1.440 | 1.884 |
| | 60 | | | | | | 0.007 | 0.177 | 0.990 | 1.400 | 1.849 |
| | 100 | | | | | | | 0.17 | 0.980 | 1.390 | 1.841 |
| | 150 | | | | | | | | 0.810 | 1.220 | 1.671 |
| | 160 | | | | | | | | | 0.410 | 0.861 |
| | 200 | | | | | | | | | | 0.447 |

3.11 Modification of the setup for experimental validation

Test results obtained on the electronically controlled inertia setup need to be validated against results obtained on a test setup using mechanical inertia of a flywheel. For this purpose, experimental setup of electronically controlled inertia, described in Section 3.8, was modified to provide a flywheel attachment is shown in Fig. 3.18. A special guard casing has been fitted to avoid accident. Flywheels with mass of 3.3 kg, 6.6 kg, 10.0 kg, and 19.6 kg can be interchangeably fitted on the shaft inside the guard

casing. All these flywheels have 0.11 m radius. Three plummer blocks are used for fitment of flywheel. Plummer block is a bearing housing device used for fitting the bearing and holding in proper position. Flywheel is mounted in between two plummer blocks. This arrangement eliminates the danger of detachment of the flywheel from the test setup during the operation of the test rig. During testing with this setup, motor is used as prime mover to obtain the set speed and then power is cutoff. For operation with electronically controlled inertia, the flywheel attachment is removed. One plummer block gets removed and two plummer blocks remain connected to the motor shaft. The setup after removing the flywheel is shown in Fig 3.19. We refer to electronically controlled inertia setup as ECI and mechanical inertia setup as MI in further description.

Fig. 3.18 Photograph of test setup with flywheel mounted for verification of the system.

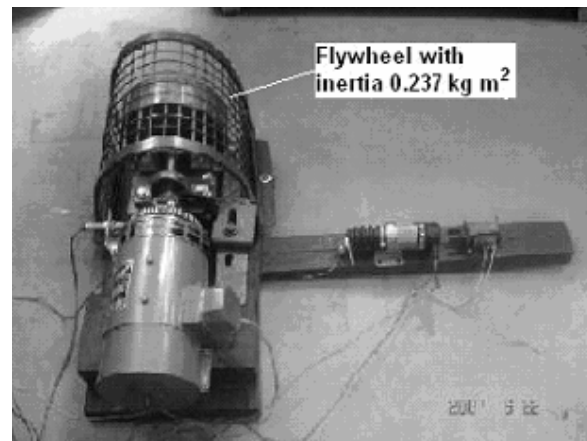
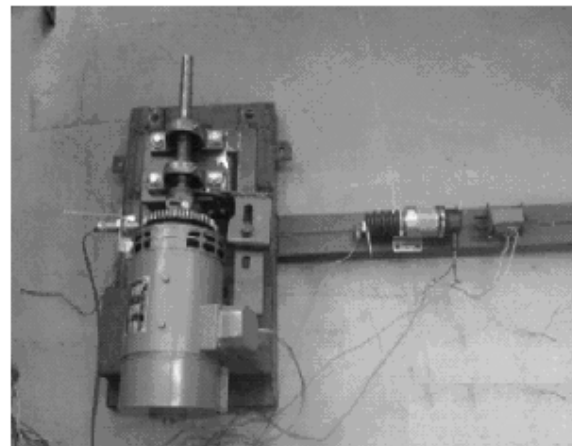


Fig. 3.19 Photograph of modified test setup to carry out experiment with different sizes of flywheel and electronic test system.



For testing of brake using MI setup, the program earlier developed for ECI setup was modified. The flywheel is accelerated to the set speed, and the brake is applied and electric supply to drive unit is disconnected. Brake release timer gets started after

application of brake. Instantaneous torque is calculated from the entered value of the inertia of the flywheel and deceleration is calculated from derivative of sensed angular speed at every sampling instant. From instantaneous values of torque and angular speed, instantaneous value of power is calculated, and used for calculating the energy dissipated in brake. When set value of dissipated energy is achieved, brake gets released.

Chapter 4

TESTS AND RESULTS

4.1 Introduction

Several tests were carried out for experimental verification of the electronically controlled inertia (ECI) setup for brake testing. First operation of ECI setup was verified against operation of a setup with mechanical inertia (MI) as described in Section 3.11. Testing was carried with the MI setup for different energy set levels, with the help of different flywheels and different angular speeds. Tests were conducted with ECI setup for the same energy levels, corresponding values of electronically controlled inertia and angular speeds, for comparing results with these from MI setup. Subsequently, the ECI setup was tested for various combinations of parameters values, for different values of energy dissipation. The test system is further used to dissipate the different values of energy levels for different values of damping and friction. Measured parameters (speed and torque), calculated parameters (deceleration, power, energy dissipated) were recorded at sampling frequency of 50 Hz. Tests were carried out by keeping angle of inclination zero and a constant brake application force. In all, six tests were carried out.

i) *Test I:* This test was carried out to verify the ECI setup against MI setup described in Section 3.11. Tests were conducted with the MI setup with two flywheels with different inertia values. Braking time t_{eb} for dissipating different values of energy was observed. During the brake operation, speed variation with time was recorded, which is used for plotting speed and deceleration with time. These tests were performed for different values of speed. Same tests were conducted using ECI setup, with corresponding values of inertia.

ii) *Test II:* This test was conducted to study the effect of electronically controlled inertia J . Friction and damping were kept zero. Speed and energy to be dissipated were

kept constant. Inertia J was varied, and braking time t_{eb} was observed for different values of J .

iii) *Test III*: This test was conducted to study the effect of speed N_s . Friction T_f and damping b were kept zero. Inertia J and energy to be dissipated E_s , were kept constant. Set speed N_s was varied, and braking time t_{eb} was observed for different values of N_s .

iv) *Test IV*: This test was conducted to study the effect of energy dissipated in brake E_s . Friction T_f and damping b were kept zero. Speed N_s and inertia J were kept constant. Energy dissipated E_s was varied, and braking time t_{eb} was observed.

v) *Test V*: This test was conducted to study the effect of friction T_f . Damping b was kept zero. Speed N_s , energy to be dissipated in brake E_s , and inertia J were kept constant. Friction torque T_f was varied, and braking time t_{eb} was observed for different values of T_f .

vi) *Test VI*: This test was conducted to study the effect of damping b . Friction T_f was kept zero. Speed N_s , energy to be dissipated in brake E_s , and inertia J were kept constant. Damping coefficient b was varied, and braking time t_{eb} was observed for different values of b .

The results for these tests are presented in the following sections.

4.2 Test I: Comparison of ECI and MI test setup

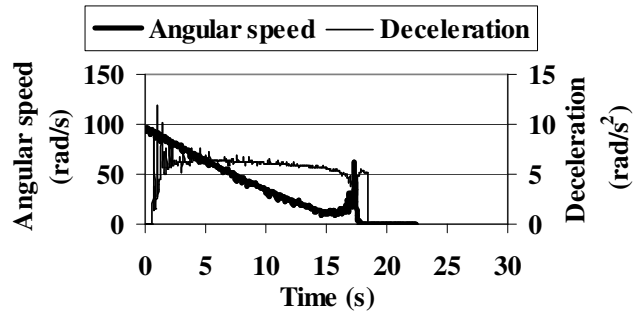
In this test, braking time is recorded using the MI setup for different values of flywheel inertia, and angular speed with zero damping and friction. Same test is repeated on the ECI setup. Values of brake release time t_{eb} recorded with the two setups are given in Table 4.1. We see that the values with the two setups closely match.

Table 4.1 Results of Test I: Braking time with flywheel and with test system for different values of inertia, angular speed and energy levels

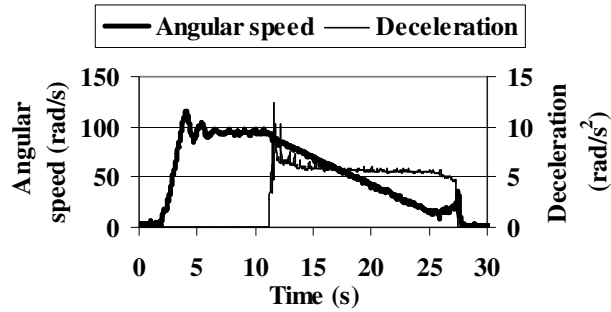
| Test No. | J (kg m ²) | N_s (rev./min.) | E_s (J) | t_{eb} (s) | | Difference (%) |
|----------|--------------------------|-------------------|-----------|--------------|----------|----------------|
| | | | | With MI | With ECI | |
| 1 | 0.237 | 900 | 1052 | 17.98 | 17.45 | 2.95 |
| 2 | 0.121 | 900 | 537 | 9.22 | 9.36 | -1.51 |
| 3 | 0.121 | 1200 | 954 | 11.09 | 11.08 | 0.09 |
| 4 | 0.121 | 900 | 400 | 4.66 | 4.70 | -0.86 |
| 5 | 0.121 | 900 | 150 | 1.41 | 1.41 | 0 |

For comparing the dynamics of the braking with the two setups, the speed and deceleration as a function of time were recorded and plotted. In case of ECI, power, energy, and torque were also plotted as a function of time. The plots for first three of the tests conducted in Table 4.1 are shown in Fig. 4.1, Fig. 4.2, and Fig. 4.3. The results of the two setups closely match. It is observed that with ECI setup energy dissipated in brake can be controlled accurately. These results indicate that ECI setup is appropriately simulating the mechanical inertia of the flywheel in transferring energy for dissipation in braking.

(a) MI setup:
 $N_s = 900 \text{ rev./min.}$,
 $J = 0.237 \text{ kg m}^2$,
 $t_{eb} = 17.98 \text{ s}$



(b) ECI setup:
 $N_s = 900 \text{ rev./min.}$,
 $J = 0.237 \text{ kg m}^2$,
 $t_{eb} = 17.45 \text{ s}$



(c) ECI setup:
 $N_s = 900 \text{ rev./min.}$,
 $J = 0.237 \text{ kg m}^2$,
 $t_{eb} = 17.45 \text{ s}$

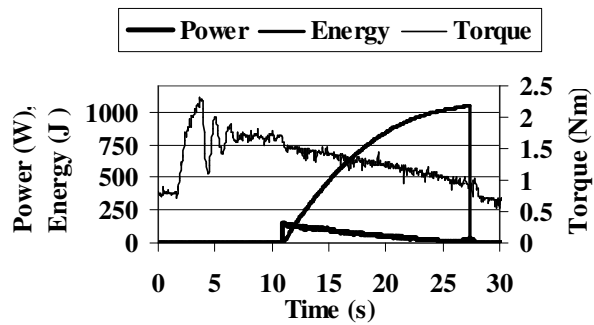
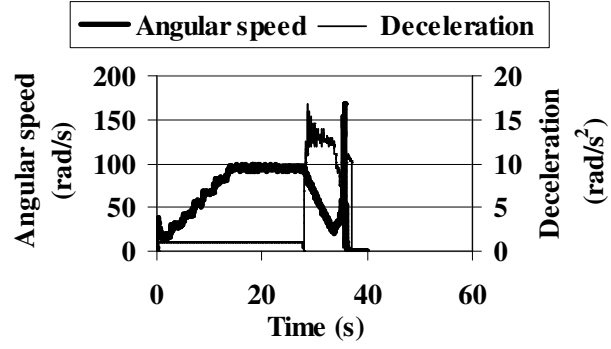
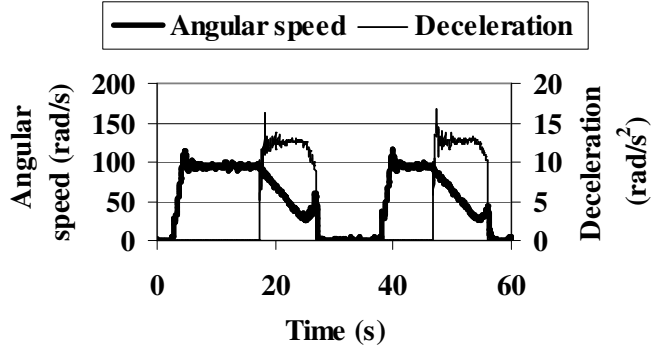


Fig. 4.1 Measured results of Test No.1. (a) Angular speed and deceleration as function of time for MI setup. (b) Angular speed and deceleration as function of time for ECI setup. (c) Power, energy and torque as function of time for ECI setup. *Test no. 1:* $J = 0.237 \text{ kg m}^2$, $N_s = 900 \text{ rev./min.}$, $E_s = 1252 \text{ J}$. Braking time (t_{eb}) recorded as: 17.98 s for MI and 17.45 s for ECI.

(a) MI setup:
 $N_s = 900 \text{ rev./min.}$,
 $J = 0.121 \text{ kg m}^2$,
 $t_{eb} = 9.22 \text{ s}$



(b) ECI setup:
 $N_s = 900 \text{ rev./min.}$,
 $J = 0.121 \text{ kg m}^2$,
 $t_{eb} = 9.36 \text{ s}$



(c) ECI setup:
 $N_s = 900 \text{ rev./min.}$,
 $J = 0.121 \text{ kg m}^2$,
 $t_{eb} = 9.36 \text{ s}$

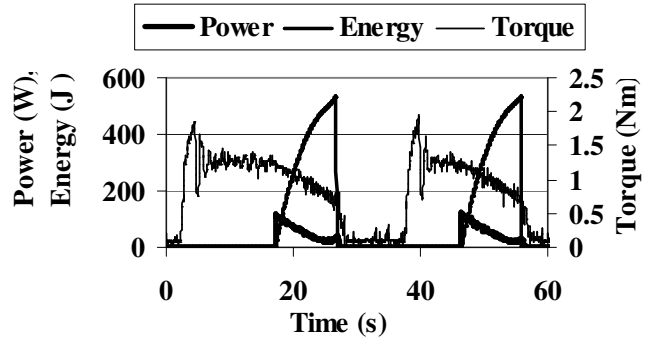
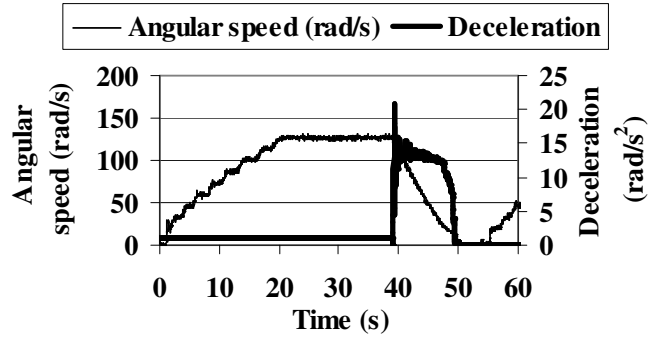
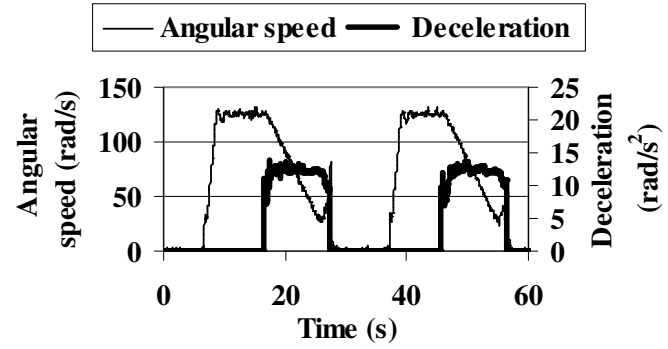


Fig. 4.2 Measured results of Test No. 2. (a) Angular speed and deceleration as function of time for MI setup. (b) Angular speed and deceleration as function of time for ECI setup. (c) Power, energy and torque as function of time for ECI setup. *Test no. 2:* $J = 0.121 \text{ kg m}^2$, $N_s = 900 \text{ rev./min.}$, $E_s = 537 \text{ J}$. Braking time (t_{eb}) recorded as: 9.22 s for MI and 9.36 s for ECI.

(a) MI setup:
 $N_s = 1200 \text{ rev./min.}$,
 $J = 0.121 \text{ kg m}^2$,
 $t_{eb} = 11.08 \text{ s}$



(b) ECI setup:
 $N_s = 1200 \text{ rev./min.}$,
 $J = 0.121 \text{ kg m}^2$,
 $t_{eb} = 11.09 \text{ s}$



(c) ECI setup:
 $N_s = 1200 \text{ rev./min.}$,
 $J = 0.121 \text{ kg m}^2$,
 $t_{eb} = 11.09 \text{ s}$

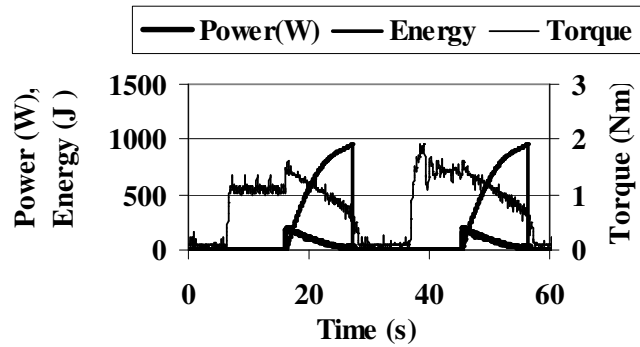


Fig. 4.3 Measured results of Test No. 3. (a) Angular speed and deceleration as function of time for MI setup. (b) Angular speed and deceleration as function of time for ECI setup. (c) Power, energy and torque as function of time for ECI setup. *Test no. 3:* $J = 0.121 \text{ kg m}^2$, $N_s = 1200 \text{ rev./min.}$, $E_s = 594 \text{ J}$. Braking time (t_{eb}) recorded as: 11.08 s for MI and 11.09 s for ECI.

4.3 Test II: Effect of variation in inertia

Value of speed N_s , energy to be dissipated E_s were kept constant, with zero damping and friction. Moment of inertia J was varied and braking time t_{eb} was recorded. Set parameters (E_s , N_s , damping coefficient b , friction torque T_f) and braking time t_{eb} for different values of moment of inertia J are given in Table 4.2. Graph of moment of inertia vs. braking time is shown in Fig. 4.4. From Fig. 4.4 it is seen that as, the moment of inertia increases, time required to dissipate the energy in brake decreases.

Total energy E_T is calculated from set energy E_s , residual energy E_{res} , energy due motor shaft inertia E_r , with damping constant $b = 0$, and friction constant $T_f = 0$ as

$$E_T = E_s + E_{res} + E_r \quad (4.1)$$

In this test system, total inertia to be simulated is summation of inertia of the rotor and inertia developed by test system. As inertia of the rotor of the motor is very small, so inertia due to shaft of the motor is kept zero throughout the experiment.

Total energy E_T in J is calculated from the set moment of inertia J in kg m^2 as

$$E_T = \frac{1}{2} J \omega_s^2 \quad (4.2)$$

where the angular speed ω_s in rad/s is calculated from set speed N_s rev./min.

$$\omega_s = 2\pi N_s / 60 \quad (4.3)$$

From (4.1), (4.2), and (4.3), we get the residual energy E_{res} in J as

$$E_{res} = \frac{1}{2} J (2\pi N_s / 60)^2 - E_s \quad (4.4)$$

Table 4.2 Results of Test II: Braking time t_{eb} for different values of moment of inertia J , for a given set of E_s , N_s , b , T_f .

| $E_s = 500 \text{ J}, b = 0, T_f = 0, N_s = 1000 \text{ rev./min.}$ | | | | | | |
|---|-------|-------|-------|-------|-------|-------|
| J (kg m^2) | 0.121 | 0.179 | 0.237 | 0.295 | 0.353 | 0.452 |
| t_{eb} (s) | 5.406 | 4.500 | 4.141 | 4.125 | 3.922 | 3.750 |

Total energy to set value of inertia is calculated from (4.1). Residual energy is calculated from (4.4). For different values of J , the recorded residual energy and the calculated value of the residual energy are given in Table 4.3. It is observed that difference between actual and calculated residual energy is less than $\pm 1\%$.

Table 4.3 Results of Test II: Calculated parameters (total energy, residual energy) and recorded readings (energy dissipated in brake and residual energy) for different values of moment of inertia J , for a given set of E_S , N_S , b , T_f .

| $E_S = 500 \text{ J}$, $b = 0$, $T_f = 0$, $N_S = 1000 \text{ rev./min.}$ | | | | | |
|--|-----------------------------------|--------------------------------------|--|--|----------------|
| Moment of inertia J (kg m^2) | Calculated total energy E_T (J) | Energy dissipated recorded E_S (J) | Residual energy recorded E_{res} (J) | Calculated residual energy E_{res} (J) | Difference (%) |
| 0.121 | 662 | 501 | 161 | 162 | 0.61 |
| 0.179 | 979 | 502 | 477 | 479 | 0.42 |
| 0.237 | 1297 | 500 | 797 | 797 | 0.00 |
| 0.295 | 1614 | 501 | 1113 | 1114 | 0.09 |
| 0.353 | 1931 | 502 | 1429 | 1431 | 0.14 |
| 0.411 | 2248 | 502 | 1746 | 1748 | 0.11 |
| 0.452 | 2473 | 501 | 1972 | 1973 | 0.05 |

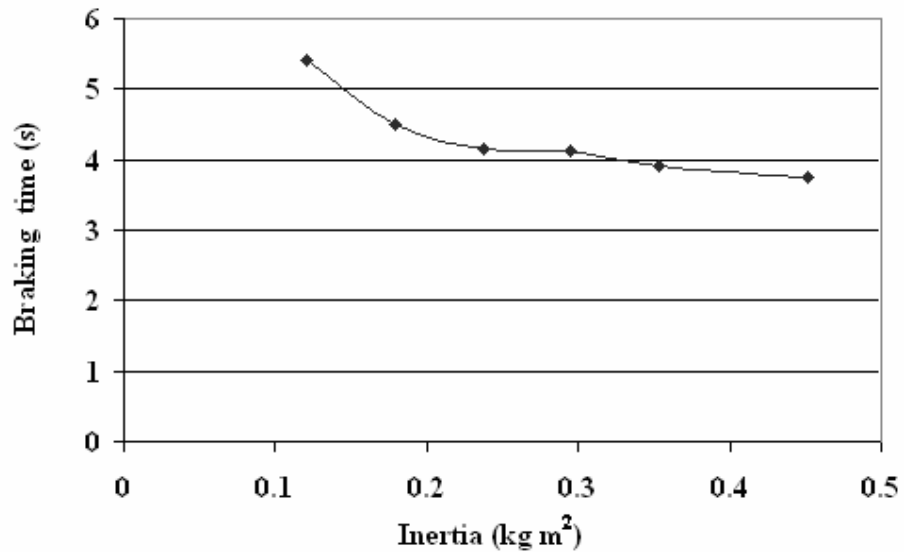


Fig. 4.4 Graph of moment of inertia vs. braking time

4.4 Test III: Effect of variation in speed

In this test, braking time t_{eb} was recorded for different values of speed N_S , by keeping the constant values of moment of inertia J and energy to be dissipated in brake E_S , with zero damping and friction. Braking time t_{eb} for different values of speed N_S are given in Table 4.4. Graph of angular speed vs. braking time is shown in Fig. 4.5. From Fig. 4.5 it is seen that, as angular speed increases, time required to dissipate the energy in brake decreases.

Total energy due to set value of speed is calculated from (4.1). Residual energy is calculated from (4.4). For different values of N_S , the recorded residual energy and the calculated value of the residual energy are given in Table 4.5. From the reading it is observed that difference between actual and calculated residual energy is less than $\pm 1.5 \%$.

Table 4.4 Results of Test III: Braking time t_{eb} for different values of speed N_S , for a given set of E_S, J, b, T_f .

| $E_S = 500 \text{ J}, J = 0.237 \text{ kg m}^2, b = 0, T_f = 0$ | | | | | | |
|---|-------|-------|-------|-------|-------|-------|
| N_S (rev./min.) | 700 | 800 | 900 | 1000 | 1100 | 1200 |
| t_{eb} (s) | 7.219 | 5.485 | 4.578 | 3.984 | 3.328 | 3.094 |

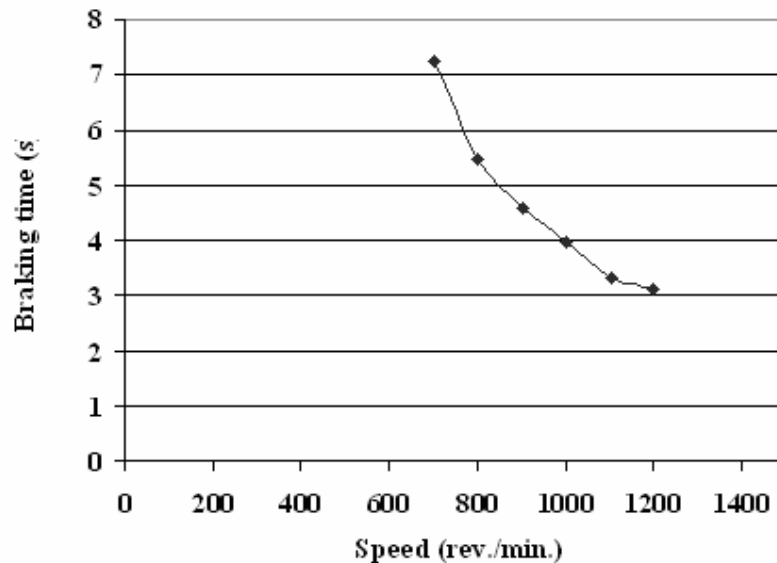


Fig. 4.5 Graph of speed vs. braking time

Table 4.5 Results of Test III: Calculated parameters (total energy, residual energy) and recorded readings (energy dissipated in brake and residual energy) for different values of speed N_S , for a given set of E_S, J, T_f .

| $E_S = 500 \text{ J}, b = 0, T_f = 0, J = 0.237 \text{ kg m}^2$ | | | | | |
|---|--|---|---|---|-------------------|
| Speed N_S (rev./min.) | Calculated total energy E_T (J) | Energy dissipated recorded E_S (J) | Residual energy recorded E_{res} (J) | Calculated residual energy E_{res} (J) | Difference (%) |
| 700 | 636 | 502 | 134 | 136 | 1.50 |
| 800 | 830 | 503 | 327 | 330 | 0.91 |
| 900 | 1051 | 501 | 550 | 551 | 0.18 |
| 1000 | 1298 | 502 | 796 | 798 | 0.25 |
| 1100 | 1570 | 500 | 1070 | 1070 | 0.00 |
| 1200 | 1869 | 501 | 1368 | 1369 | 0.07 |

4.5 Test IV: Effect of variation in energy

In this test, braking time t_{eb} was recorded for different values of energy E_S , by keeping the constant values of moment of inertia J and speed N_S , with zero damping and friction. Braking time t_{eb} for different values of speed E_S are given in Table 4.6. Graph of energy vs. braking time is shown in Fig. 4.6. From Fig. 4.6 it is seen that, as net energy to be dissipated increases, time required to dissipate the energy in brake increases.

Total energy due to set value of speed is calculated from (4.1). Residual energy is calculated from (4.4). For different values of E_S , the recorded residual energy and the calculated value of the residual energy are given in Table 4.7. From the reading it is observed that difference between actual and calculated residual energy is less than $\pm 2.5 \%$.

Table 4.6 Results of Test IV: Braking time t_{eb} for different values of energy E_S , for a given set of N_S, J, b, T_f .

| $J = 0.237 \text{ kg m}^2, b = 0, T_f = 0, N_S = 1000 \text{ rev./min.}$ | | | | | | |
|--|-------|-------|-------|-------|--------|--------|
| E_S (J) | 700 | 800 | 900 | 1000 | 1100 | 1200 |
| t_{eb} (s) | 5.787 | 6.532 | 7.297 | 9.078 | 10.219 | 11.875 |

Table 4.7 Results of Test IV: Calculated parameters (total energy, residual energy) and recorded readings (energy dissipated in brake and residual energy) for different values of energy E_S , for a given set of N_S , J , T_f .

| $J = 0.237 \text{ kg m}^2, b = 0, T_f = 0, N_S = 1000 \text{ rev./min.}$ | | | | | |
|--|--|---|---|---|-------------------|
| Energy E_S (J) | Calculated total energy E_T (J) | Energy dissipated recorded E_S (J) | Residual energy recorded E_{res} (J) | Calculated residual energy E_{res} (J) | Difference (%) |
| 700 | 1298 | 701 | 597 | 598 | 0.17 |
| 800 | 1298 | 802 | 496 | 498 | 0.40 |
| 900 | 1298 | 902 | 396 | 398 | 0.50 |
| 1000 | 1298 | 1002 | 296 | 298 | 0.67 |
| 1100 | 1298 | 1103 | 195 | 198 | 1.52 |
| 1200 | 1298 | 1202 | 96 | 98 | 2.04 |

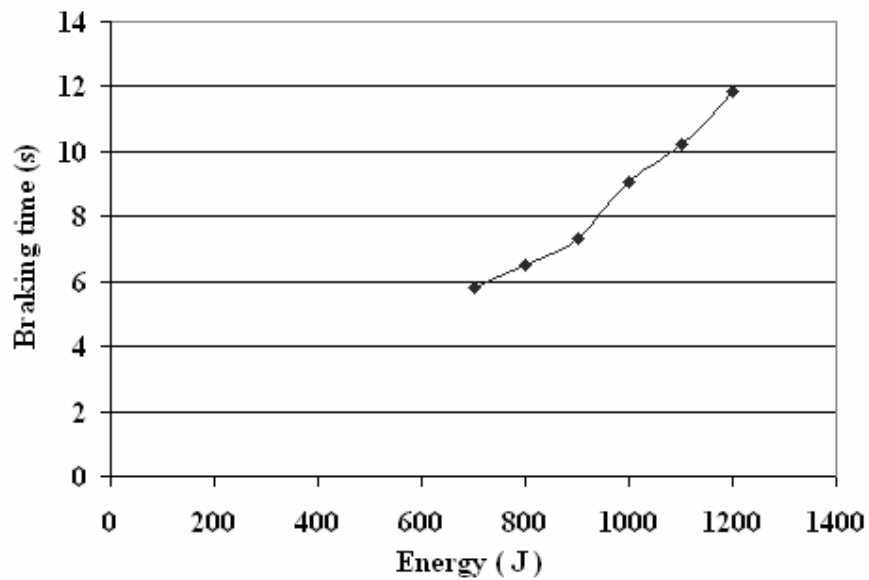


Fig. 4.6 Graph of energy vs. braking time

4.6 Test V: Effect of variation in friction

In this test, braking time t_{eb} was recorded for different values of friction constant T_f , by keeping the constant values of moment of inertia J and speed N_S , energy E_S with zero damping. Braking time for different values of friction constant T_f are given in Table 4.8.

Graph of friction vs. braking time is shown in Fig. 4.7. From Fig. 4.7 it is seen that as, friction increases, time required to dissipate the energy in brake increases.

Table 4.8 Results of Test V: Braking time t_{eb} for different values of friction constant T_f , for a given set of N_S, J, b, E_S .

| $J = 0.237 \text{ kg m}^2, b = 0, E_S = 500 \text{ J}, N_S = 1000 \text{ rev./min.}$ | | | | | | |
|--|-------|-------|-------|-------|-------|-------|
| T_f | 0.05 | 0.10 | 0.20 | 0.30 | 0.40 | 0.50 |
| $t_{eb} \text{ (s)}$ | 3.509 | 3.635 | 3.812 | 3.873 | 3.944 | 4.000 |

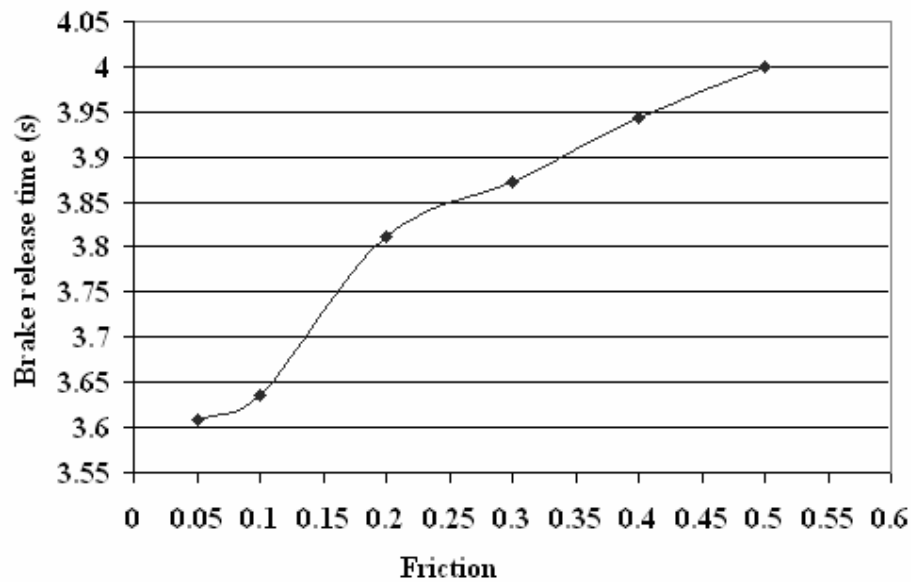


Fig. 4.7 Graph of friction vs. braking time

4.7 Test VI: Effect of variation in damping

In this test, braking time t_{eb} was recorded for different values of damping b , by keeping the constant values of moment of inertia J and speed N_S , energy E_S with zero friction. Braking time for different values of damping b is given in Table 4.9. Graph of damping vs. braking time is shown in Fig. 4.8. From Fig. 4.8 it is seen that as, damping increases, time required to dissipate the energy in brake increases.

Table 4.9 Results of Test VI: Braking time t_{eb} for different values of damping b , for a given set of N_s, J, T_f, E_s .

| $J = 0.237 \text{ kg m}^2, T_f = 0, E_s = 500 \text{ J}, N_s = 1000 \text{ rev./min.}$ | | | | | | |
|--|--------|--------|--------|--------|--------|--------|
| $b \text{ (Nm s)/rad}$ | 0.0004 | 0.0011 | 0.0016 | 0.0021 | 0.0027 | 0.0032 |
| $t_{eb} \text{ (s)}$ | 3.610 | 3.735 | 3.797 | 3.812 | 3.828 | 3.860 |

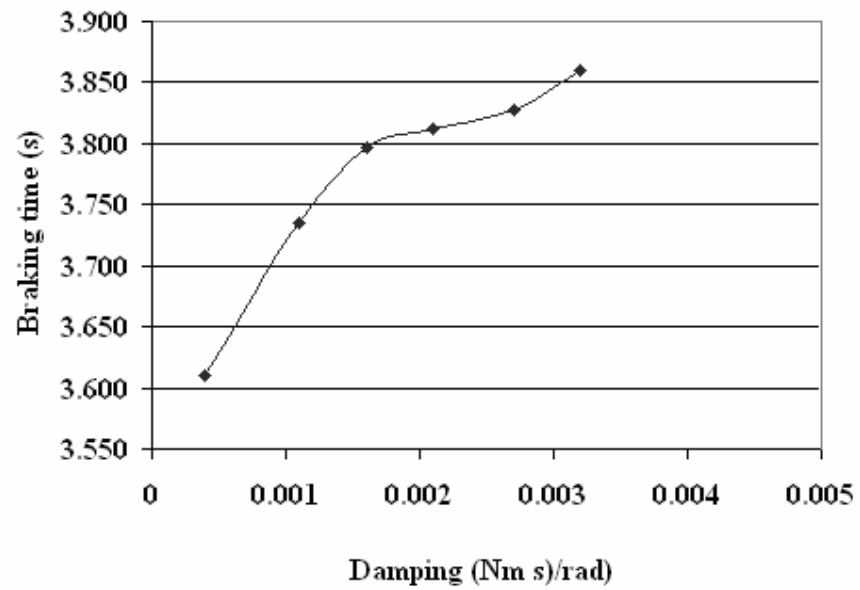


Fig. 4.8 Graph of damping vs. braking time

Chapter 5

SUMMARY AND CONCLUSIONS

Laboratory testing of brake and clutch system is generally conducted on inertia dynamometer equipped with a drive motor and a detachable flywheel, which represents the tractor mass. It is unsafe to rotate the mass at higher speed. Further there is a high wear and tear of the system. It is difficult to generate variable inertia as it involves changing the flywheel. Further, simulation of variable damping forces and friction forces is not possible on these setups. In order to overcome these drawbacks of the inertia dynamometer, there is a need to develop a test bench which can develop variable inertia, damping, and friction. Objectives of this project were to develop an electronically controlled setup for laboratory testing of brakes and clutches with following features

- (a) Simulation of variable moment of inertia, damping, and friction.
- (b) Elimination of risks due to flywheel.
- (c) Electronic control of energy dissipated per braking cycle, independent of braking force and type of brake surface.
- (d) Monitoring and recording the time taken for dissipating a specified amount of energy in the brake.
- (e) Monitoring and recording various parameters related to braking: speed, deceleration, torque, power, and cumulative dissipated energy as a function of time.
- (f) Faster testing

A 0.746 kW (1 H. P.) separately excited dc motor with electronically controlled drive unit, speed and current sensors, and an industrial PC with a data acquisition board have been used for developing a test setup for concept demonstration. Speed and current sensors with amplifiers are used to give motor speed and current feedback to control unit. Values of moment of inertia, damping coefficient, friction torque, and starting

speed can be set through potentiometers connected to the analog inputs of data acquisition board. Drive unit is used to control the speed of the dc motor. Brake to be tested is mounted on the motor shaft: Braking is controlled through a solenoid. All these signals are interfaced to computer through data acquisition card. User interface screens are developed in NI Labview package.

The total torque T coming on the motor shaft is sum of the torque due to moment of inertia T_i , torque due to damping T_d , torque due to kinetic friction T_{fr} , and torque due to gravitation. Software adjusts the control signal to the drive unit, to get required torque. Instantaneous values of measured signals like speed and current and calculated parameters like power, angular velocity, deceleration, energy dissipated etc are online calculated from values of speed, current, and time and these are recorded in a file with predefined data acquisition rate.

The operation of the setup with electronically controlled inertia (ECI) was verified against a setup with mechanical inertia (MI). Values of the braking time, using the two setups for dissipation of specific value of energy for a given brake, closely matched. The decelerations plotted as a function of time also closely matched. Hence we conclude that ECI setup appropriately simulated the mechanical inertia of the flywheel in transferring energy during braking. Five other sets of tests were carried out to check the system operation, for varying (a) moment of inertia J , (b) set speed N_s , (c) energy to be dissipated per cycle E_s , (d) friction constant T_f , and (e) damping coefficient b , one at a time. In all these tests, an appropriate variation in the braking time with respect to parameter variation was observed. Further the obtained values of residual energy (energy remaining in the flywheel at the end of braking) closely matched with the calculated values.

From the above results, we may conclude that the implementation of electronically controlled setup for laboratory testing of brakes and clutches has been successful, at the level of concept demonstration. The electronic monitoring and control setup can be used for devising a test rig for testing tractor brakes and clutches.

Appendix A

DATA ACQUISITION CARD AND DRIVE UNIT

NI 6221 (68-Pin)

| | | | |
|-------------|----|----|-------------|
| AI 0 | 68 | 34 | AI 8 |
| AI GND | 67 | 33 | AI 1 |
| AI 9 | 66 | 32 | AI GND |
| AI 2 | 65 | 31 | AI 10 |
| AI GND | 64 | 30 | AI 3 |
| AI 11 | 63 | 29 | AI GND |
| AI SENSE | 62 | 28 | AI 4 |
| AI 12 | 61 | 27 | AI GND |
| AI 5 | 60 | 26 | AI 13 |
| AI GND | 59 | 25 | AI 6 |
| AI 14 | 58 | 24 | AI GND |
| AI 7 | 57 | 23 | AI 15 |
| AI GND | 56 | 22 | AO 0 |
| AO GND | 55 | 21 | AO 1 |
| AO GND | 54 | 20 | NC |
| D GND | 53 | 19 | P0.4 |
| P0.0 | 52 | 18 | D GND |
| P0.5 | 51 | 17 | P0.1 |
| D GND | 50 | 16 | P0.6 |
| P0.2 | 49 | 15 | D GND |
| P0.7 | 48 | 14 | +5 V |
| P0.3 | 47 | 13 | D GND |
| PFI 11/P2.3 | 46 | 12 | D GND |
| PFI 10/P2.2 | 45 | 11 | PFI 0/P1.0 |
| D GND | 44 | 10 | PFI 1/P1.1 |
| PFI 2/P1.2 | 43 | 9 | D GND |
| PFI 3/P1.3 | 42 | 8 | +5 V |
| PFI 4/P1.4 | 41 | 7 | D GND |
| PFI 13/P2.5 | 40 | 6 | PFI 5/P1.5 |
| PFI 15/P2.7 | 39 | 5 | PFI 6/P1.6 |
| PFI 7/P1.7 | 38 | 4 | D GND |
| PFI 8/P2.0 | 37 | 3 | PFI 9/P2.1 |
| D GND | 36 | 2 | PFI 12/P2.4 |
| D GND | 35 | 1 | PFI 14/P2.6 |

NC = No Connect

Fig. A.1 68 - pin D connector of data acquisition card NI 6221 (from National Instruments)



Fig. A.2 Photograph of data acquisition card, National Instrument model NI 6221.

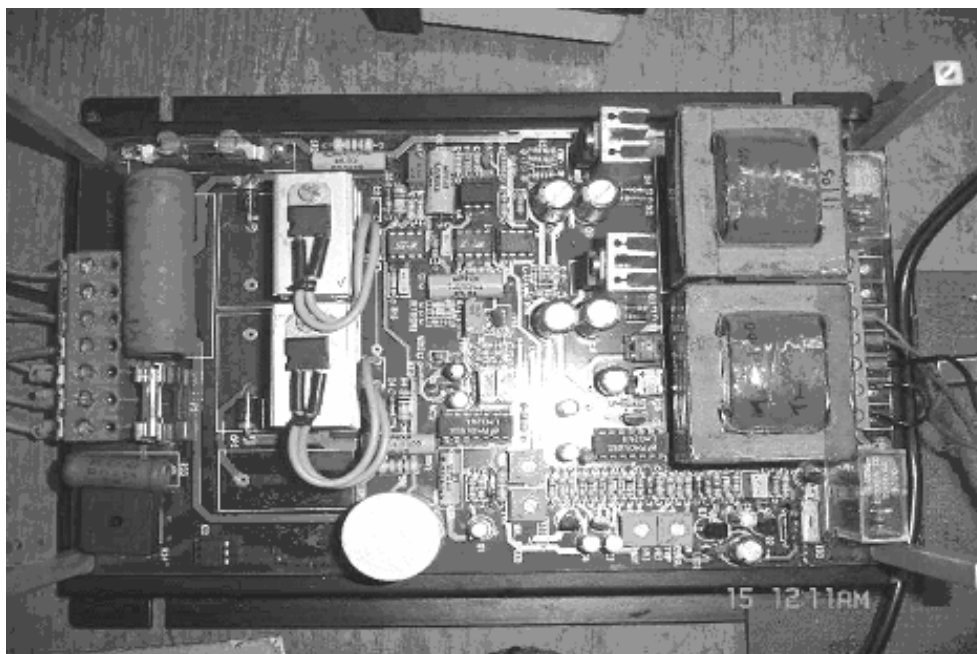


Fig. A.3 Drive for separately excited dc motor, Libratherm model TDM -1000.

Appendix B

TESTING OF DATA ACQUISITION CARD

B.1 Testing of analog input in NI 6221 driver software

NI 6221 card has 16 analog inputs. Eight of these inputs are used in test system. All 16 analog inputs were checked through NI 6221 driver software test panel. Following settings were made in the driver software test panel for checking the analog input channels: i) Channel number: to which analog input voltage signal is given ii) Maximum input limit of signal iii) Minimum input limit of signal. iv) Rate: the sampling rate of the card. v) Input configuration: the type of input signal. After these settings, input voltage signal is applied to the selected analog input channel and start button is pressed. The value and graphical representation of the applied signal gets displayed on the panel. This process was followed for each of the channels. Test panel screen for testing of analog input channels in NI 6221 driver software is shown in Fig. B.1.

B.2 Testing of analog output in NI 6221 driver software

NI 6221 card has 2 analog outputs. One of these is used in the test system. Each of the analog outputs was checked through the NI 6221 driver software test panel. Following settings were made for checking the analog output channels: i) Channel name ii) Maximum output limit iii) Minimum output limit. After these settings, voltage signal is output from the selected analog output channel and update button is pressed. The output voltage sourced from analog output channel is measured on a multimeter. Test panel screen for testing of analog output channel in NI 6221 driver software is shown in Fig. B.2.

B.3 Testing of digital input and output in NI 6221 driver software

NI 6221 card has 10 programmable digital I / O lines. Out of these lines digital signals one digital output is used in our test system. All the digital outputs were checked through NI 6221 driver software test panel. Following settings were made: i) Port name ii) Select direction: Set the signal as digital input or digital output iii) Select state: Set the digital signal as low or high. The selected state mode was set high and low output voltage was measured with the help of a multimeter. Test panel screen for testing of digital channel in NI 6221 drive software is shown in Fig. B.3.

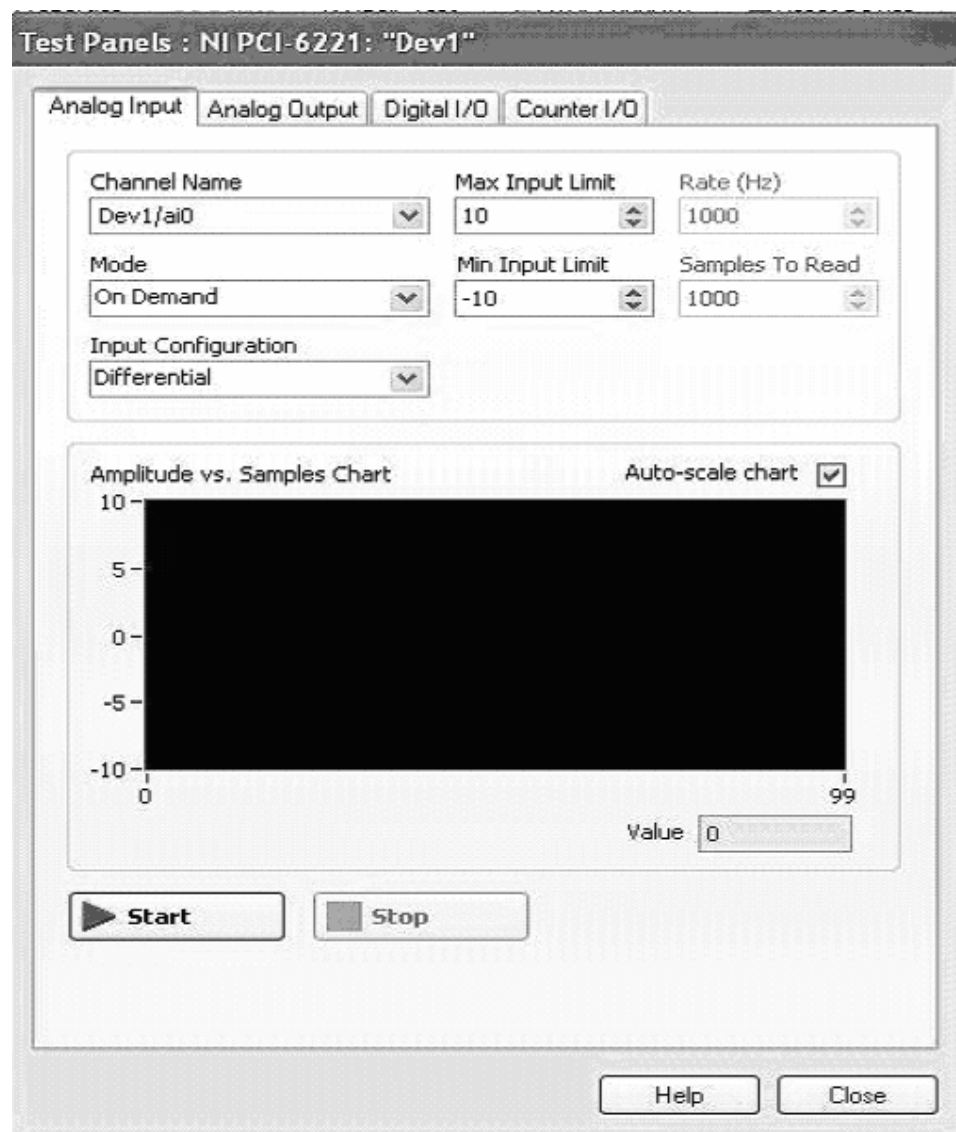


Fig. B.1 Testing of analog input in NI 6221 driver software.

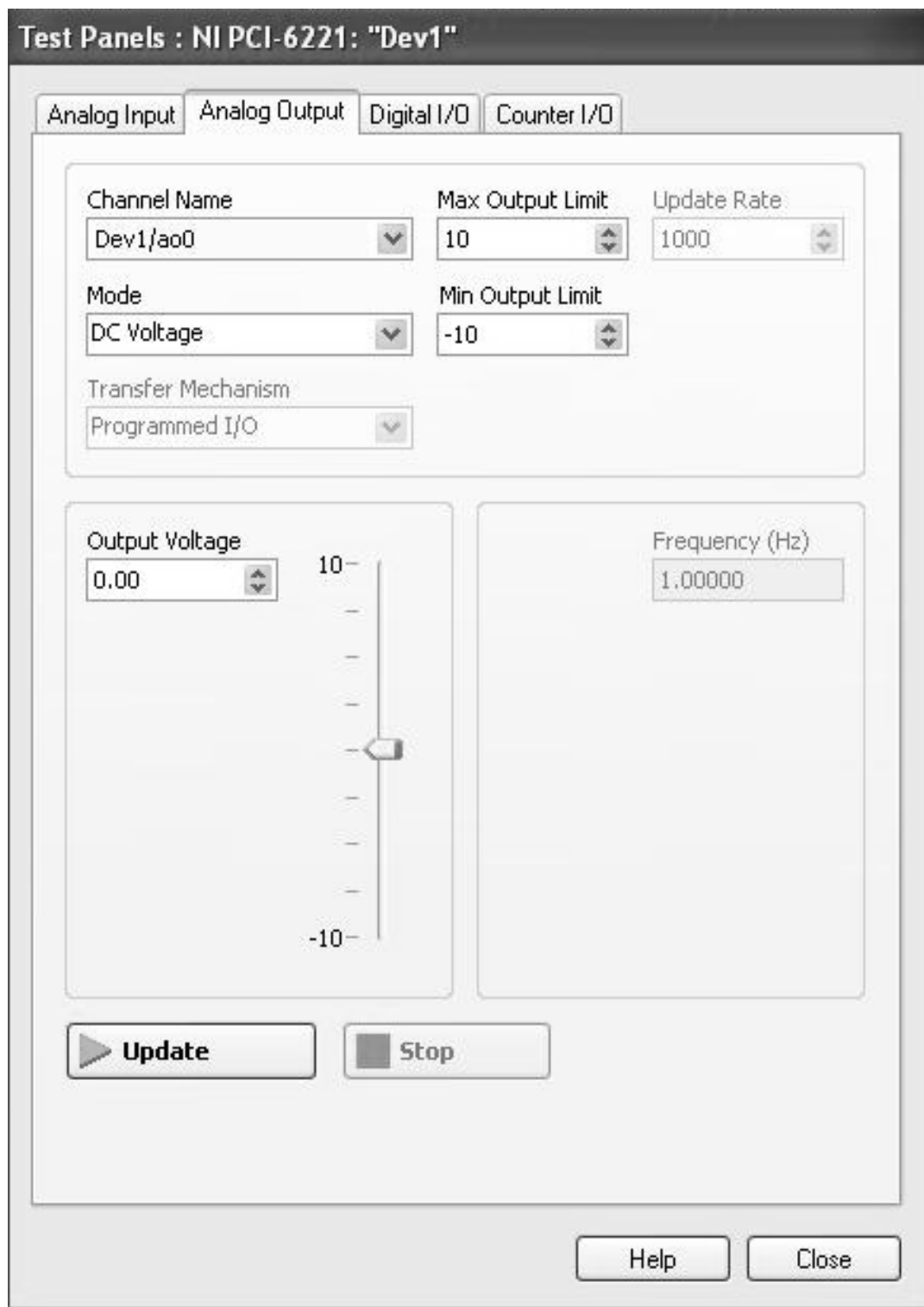


Fig. B.2 Testing of analog output in NI 6221 driver software.

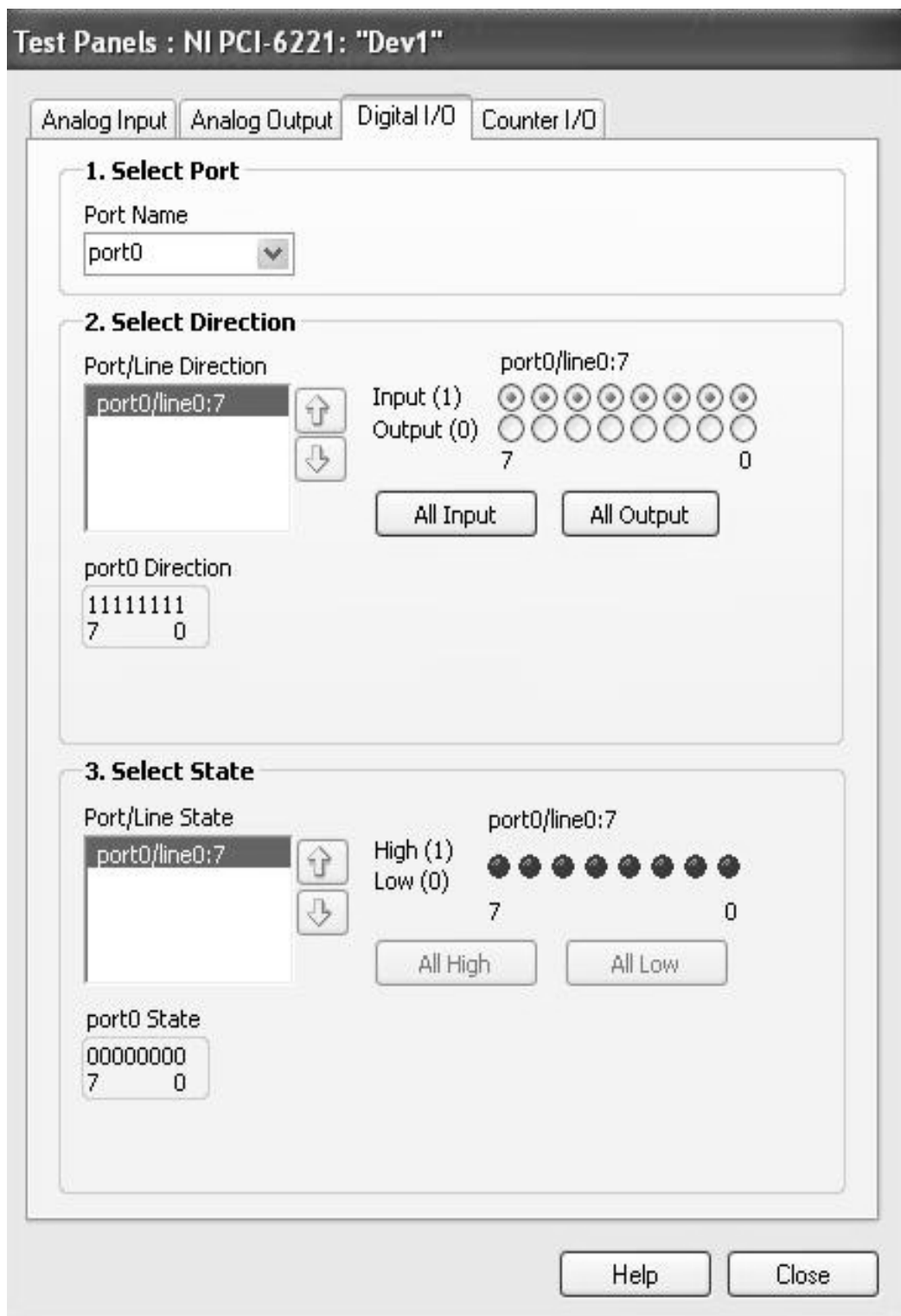


Fig. B.3 Testing of digital I / O lines in NI 6221 driver software.

Appendix C

ASSEMBLY OF TEST SYSTEM

Table C.1 Component list of test system.

| Sl. No. | Name of the component | Quantity |
|---------|--|----------|
| 1 | Separately excited dc motor 0.746 kW (1 H. P.) | 1 |
| 2 | Current sensor (0 - 5 A : 0 - 75 mV) | 1 |
| 3 | Current amplifier (0 - 75 mV : 0 - 10 V) | 1 |
| 4 | Analog optoisolator: 0 - 10 V to 0 - 10 V | 1 |
| 5 | Frequency-to-voltage converter (0 - 1500 Hz : 0 - 10 V) | 1 |
| 6 | 24 V, 5 A dc power supply | 1 |
| 7 | 10 V, 1 A dc power supply | 1 |
| 8 | Potentiometer (10 k Ω) | 6 |
| 9 | Contactactor (230 V ac coil 10 A contact) | 1 |
| 10 | Data acquisition card (National Instruments 6221) | 1 |
| 11 | Computer (Dynalog IPC - 611) | 1 |
| 12 | Magnetic pulse pick up | 1 |
| 13 | 60 toothed wheel | 1 |
| 14 | Drive | 1 |
| 15 | MS connector (10 A) | 1 |
| 16 | Junction box for to interface electronic system with data acquisition card | 2 |
| 17 | Junction box for data acquisition card | 1 |

| Sl. No. | Name of the component | Quantity |
|----------------|------------------------------|-----------------|
| 18 | Brake with assembly | 1 |
| 19 | Solenoid coil (12 V dc) | 1 |
| 20 | Relay (24 V dc) | 1 |
| 21 | Optoisolator | 1 |

Appendix D

BRAKE TESTING BASED ON IS: 12061-1994 FOR MAHINDRA AND MAHINDRA TRACTOR

Brake endurance testing based on IS: 12061 - 1994 for Mahindra and Mahindra tractor is explained as follows. With this test cycle endurance testing of brake is carried out.

1. Both brake and clutch should be in release condition.
2. Increase the engine speed to predefined value.
3. Disengage the clutch.
4. Apply brake.
5. Check the axle speed and if axle speed becomes zero, increment the cycle counter and compare it with the set number of cycles. If cycle counter is less than the set number of cycles go to step 1 and repeat the cycle.

ACKNOWLEDGEMENTS

I would like to express my sincere gratitude to my supervisors, Prof. P. C. Pandey and Prof. L. R. Subramanyan, for all the support, and encouragement.

I am grateful to my family for the unfailing encouragement and support they have given me over the years. I am thankful to the authorities of Mahindra and Mahindra Limited, Mumbai for sponsoring me to M.Tech. programme at IIT Bombay and to my seniors and colleagues for all the help.

Chaitanya J. Diwan

IIT Bombay

July 2007

REFERENCES

- [1] J. J. Hine, *Tractors on the Farm: Their Choice, Use, and Maintenance*. London: Farmer and Stock Breeder, 1955.
- [2] F. R. Jones and W. H. Aldred, *Farm Power and Tractor*. New York: McGraw-Hill, 1980.
- [3] E. L. Barger and E. G. Mekibben, *Tractors and Their Power Units*. New York: John Wiley, 1952, pp. 334-344.
- [4] S. C. Jain and C. R. Rai, *Farm Tractors: Maintenance and Repair*. Delhi: Standard, 1999, pp. 186-191.
- [5] J. K. Thompson, "The use of inertia simulation in brake dynamometer testing," Available online, [http://www.linkeng.com/pdf/JEF%202002%20 Presentation.pdf](http://www.linkeng.com/pdf/JEF%202002%20Presentation.pdf), site of Link Engineering Company, [2002], downloaded on Nov. 2, 2005.
- [6] J. A. Wheeler, *Gravitation and Inertia*. Princeton, New Jersey: Princeton University, 1995.
- [7] R. Govindarajan, "Development of accelerated testing technique for evaluation of brakes for two and three wheelers," presented at *SAE Conf. Symposium on International Automotive Technology*, vol. 2, no. 2005-26-037, pp. 567-574, Pune, India, Jan. 2005.
- [8] J. Scott, "Brake performance testing and truck runaway analysis," *SAE2003. Journal of Commercial Vehicles.*, section-2, no. 2003-01-3396, pp. 236-246, 2003.
- [9] A. F. Emery, "Measured and predicted temperature of automotive brakes under heavy or continuous braking," *SAE2003. Journal of Commercial Vehicles.* section-6, no. 2003-01-2712, pp. 2338-2345, 2003.
- [10] T. P. Newcomb, *Braking of Road Vehicles*. London: Chapman and Hall, 1967.
- [11] T. P. Newcomb, *Commercial Vehicle Braking*. Boston: Butterworth, 1979.

- [12] Gaurang Infotech, "Software for engine, vehicle, and components testing," Available online, <http://www.dynomerck.com/brakein.htm>, site of Dynomerck Controls, [2001], downloaded on Nov. 1, 2005.
- [13] E. I. Rivin, *Stiffness and Damping in Mechanical Design*. New York: Marcel Dekker, 2003.
- [14] M. Cao, "Development of friction component model for automotive power train system analysis and shift controller design based on parallel modulated neural networks," *Journal of Dynamic Systems, Measurement, and Control*, vol.127, pp. 382-405, September 2005.
- [15] B. V. Budanov, "Interaction of friction and vibration," *Soviet Journal of Friction and Wear*, vol. 1, no. 1, pp. 59-67, 1981.
- [16] K. Ogata, *Modern Control Engineering*. New Delhi: Prentice-Hall, 1984, pp. 99-106.
- [17] B. C. Kuo, *Automatic Control Systems*. New Delhi: Prentice-Hall, 1991, pp. 154-190.
- [18] I. J. Nagrath and M. Gopal, *Control Systems Engineering*. New Delhi: Wiley Eastern, 1991, pp. 15-73.
- [19] J. M. Vance and B. T. Murphy, "Inertial energy storage for home or farm use based on a flexible flywheel," presented at *Flywheel Technology Symposium*, pp. 75-87, 1980.
- [20] C. M. Ong, "An analog simulation of a flywheel propulsion system for buses," presented at *Flywheel Technology Symposium*, pp. 31-144, 1980.
- [21] Y. Tessuya and Y. Takeshi, "Apparatus for testing characteristics of tractor brake," European patent No. JP60058524. April 4, 2004, Available online, <http://v3.espacenet.com/textdoc?DB=EPODOC&IDX=JP60058524&F=0>, site of European Patent Office.
- [22] T. Tetsuo and K. Takuo, "Testing method for car running using electric inertia chassis dynamometer," European patent No. JP57133335. Aug. 18, 1982, Available online, <http://v3.espacenet.com/textdoc?DB=EPODOC&IDX=JP57133335&F=0>, site of European Patent Office.
- [23] F. Gernot, "Method for simulating inertia force by dynamometer," European patent No. DE19730851. Feb. 05, 1998, Available online, <http://v3.espacenet.com>.

com/textdoc?DB=EPODOC&IDX=DE19730851&F=0, site of European Patent Office.

- [24] J. Pittner, "An improvement in or relating to constant torque and inertia control for armature current regulated dc motor with field weakening," European patent No. ZA7209161. Sept. 26, 1973, Available online, <http://v3.espacenet.com/textdoc?DB=EPODOC&IDX=ZA7209161&F=0>, site of European Patent Office.
- [25] J. F. Gieras, *Permanent Magnet Motor Technology Design and Applications*. New York: Marcel Dekker, 1997.
- [26] G. K. Dubey, *Fundamentals of Electrical Drives*. New Delhi: Narosa, 1995, pp. 60-62.
- [27] Electro-craft corporation, *DC Motors Speed Controls Servo Systems*. New York: Pergamon, 1984.
- [28] D. F. Geiger, *Phaselock Loops for DC Motor Speed Control*. New York: John Wiley, 1981.
- [29] W. Shepherd and L. N. Hulley, *Power Electronics and Motor Control*. New York: Cambridge University, 1987.
- [30] P. Emanuel, *Motors, Generators, Transformers, and Energy*. Englewood Cliffs, New Jersey: Prentice-Hall, 1985.
- [31] M. H. Rashid, *Power Electronics: Circuit, Devices, and Applications*. New Delhi: Prentice-Hall, 1994, pp. 493-500.
- [32] K. Nakano, "A CMOS rotary encoder using magnetic sensor arrays," *IEEE Sensors Journal*, vol. 5, no. 5, pp. 889-908, October 2005.
- [33] A. D. Cheok, "Fuzzy logic rotor position estimation based switched reluctance motor dsp drive with accuracy enhancement," *IEEE Trans. Power Electronics*, vol. 20, no. 4, pp. 908-921, July 2005.
- [34] J. C. Hamann, "Analysis and design of motion control system with positive force feedback using robust control methods," *IEEE Trans. Control Systems Technology*, vol. 13, no. 5, pp. 752-765, September 2005.
- [35] K. Krishnan, *Electric Motor Drives Modeling, Analysis, and Control*. Englewood Cliffs, New Jersey: Prentice-Hall, 2001.
- [36] H. Kume, *Statistical Methods for Quality Improvement*. Chennai: Productivity, 2006, pp. 68-156.